Towards a method for detecting the potential genotoxicity of nanomaterials

NANOGENOTOX

D4.5: Surface charge, hydrodynamic size and size distributions by zetametry, dynamic light scattering (DLS) and small-angle X-ray scattering (SAXS) in optimized aqueous suspensions for titanium and silicon dioxide.

Key intrinsic physicochemical characteristics of NANOGENOTOX nanomaterials

August
2012

Co-funded by
the Health Programme
of the European Union

NANOGENOTOX

Grant Agreement n° 2009 21 01

WP 4 : Physicochemical Characterisation of Manufactured Nanomaterials (MNs) and Exposure Media (EMs)

Deliverable 4.5: Nanomaterial datasets with requested physicochemical properties

Surface charge, hydrodynamic size and size distributions by zetametry, dynamic light scattering (DLS) and small-angle X-ray scattering (SAXS) in optimum aqueous suspensions for titanium and silicon dioxide

Deliverable leader : NRCWE

Keld Alstrup Jensen

The National Research Centre for the Working Environment (NRCWE),

Lersø Parkallé 105, DK-2100 Copenhagen, DENMARK

National Research Centre
for the Working Environment

Workflow	
Author(s)	**Reviewer(s)**
Camille Guiot and Olivier Spalla (CEA)	WP Leader: Keld Alstrup Jensen (NRCWE)
Keld Alstrup Jensen, Yahia Kembouche, (NRCWE)	Coordinator: Nathalie Thieriet (ANSES)
Davy Rousset and Olivier Witschger (INRS)	

Document status:	v.1	first draft	Creation date:	13/02/2011
	v.2	second draft	date:	01/05/2012
	v.3	final revision	date:	28/08/2012
	V.4	comment from NGTX coordination tea	date:	11/02/2013
	v.5	final revision by authors	date:	13/03/2013

Confidentiality level of the deliverable		
PU	Public	PU
CO	Confidential, only for members of the consortium (including the Commission Services)	

www.nanogenotox.eu

Co-funded by
the Health Programme
of the European Union

Contents

1. Introduction

This report presents the final results and description of the standard operation procedures (SOPs) for characterization of manufactured nanomaterials regarding their surface charge as function of pH as well as their size-distributions in optimal dispersed state using dynamic light scattering and scattered X-ray techniques. In addition to general data presentation, the report also contains data from an interlaboratory comparison to investigate variations between laboratories as well as to assess the vial to vial and intra-vial variability.

The results have been generated during the first two years of the Joint Actions project, NANOGENOTOX, which is funded by the EAHC (Executive Agency for Health and Consumers). Temporary results and SOPs have previously been reported in Guiot *et al.* (2010) and Jensen *et al*., (2010). This report, together with six other topical reports and a summary report officially fulfils deliverable 5 of the project, including analysis of the hydrochemical reactivity of the selected nanomaterials. The complete final report series on physico-chemical characterization are listed hereafter:

> D4.1: Summary report on primary physiochemical properties of manufactured nanomaterials used in NANOGENOTOX

> D4.2: Transmission electron characterization of NANOGENOTOX nanomaterials and comparison with and atomic force microscopy

> D4.3: Crystallite size, mineralogical and chemical purity of NANOGENOTOX nanomaterials

> D4.4: Determination of specific surface area of NANOGENOTOX nanomaterials

> D4.5: Surface charge, hydrodynamic size and size distributions by zetametry, dynamic light scattering (DLS) and small-angle X-ray scattering (SAXS) in optimum aqueous suspensions for titanium and silicon dioxide

> D4.6: Dustiness of NANOGENOTOX nanomaterials using the NRCWE small rotating drum and the INRS Vortex shaker

> D4.7: Hydrochemical reactivity, solubility, and biodurability of NANOGENOTOX MN.

Note that the results in the current report are considered the final data. The SOPs used to achieve the data are shown in Appendix A to F.

The objective of this report is to gather the main properties of raw NM in aqueous suspensions. Suspensions are prepared in a view to obtain the best state of dispersion in almost a pure aqueous medium, *i.e.* without addition of any adsorbing moiety or important concentration and variety of ions. The techniques employed for the characterizations reported here are zetametry, dynamic light scattering (DLS) and small-angle X-ray scattering (SAXS). In a spirit of concision, the sample

preparation, measurements and data treatment are only briefly reminded in the main document. Nevertheless, the full standard operating procedures (SOP) for each technique, sample preparation protocol and additional data are detailed in the appendices at the end of the document. The main results are summarized here and compared between the different NM. Extended results were reported in internal reports for NANOGENOTOX members and partly in previous NANOGENOTOX deliverable (1).

In a first part the evolution of NM surface charge over the pH range is studied by zetametry, allowing determination of isoelectric points (IEP). In a second part, two scattering techniques are then applied on well dispersed stable suspensions, which give information on intensity-related size parameters. DLS results provide a mean aggregate size and some size distributions, whereas SAXS describes more finely the average structure of fractal aggregates through a general model taking into account the radius of gyration of primary particles and of aggregates and their fractal dimension. The third part is dedicated to the validation of procedures, *i.e.* the DLS measurements performed on apparatus from different manufacturers and by different experimenters. The sub-sampling homogeneity is then assessed by DLS measurements.

2. *Properties of aqueous suspensions over the pH range*

The titania and silica NM were analyzed for surface charge as a function of pH to determine the stability properties of their aqueous suspensions over the pH range, and subsequently their iso-electric point (IEP, *i.e.* the pH at which the surface charge is globally neutral).

The reported zeta potential measurements and determinations of the isoelectric point (IEP) were performed at CEA. These data were previously reported in midterm deliverable (1) and internal reports (detailed for each NM with table of values). Sample preparation and data treatment are only briefly reminded here but are detailed in appendix A.

2.1. *Sample preparation*

Samples for zeta potential measurements are prepared as aqueous suspensions of 0.5 g/L for TiO_2 nanomaterials, and 1 g/L for Silica nanomaterials with constant ionic strength of 0.036 mol/L (monovalent salt) and controlled pH. They are prepared by dilution of concentrated sonicated stock suspensions of 10 g/L in pure water into pH and ionic strength controlled "buffers" prepared by addition of HNO_3, NaOH and $NaNO_3$ in various proportions.

2.1.1. Measurements

For each suspension of known pH, fixed ionic strength and fixed NM concentration, zeta potential is measured on a general purpose mode with automatic determination of measurement parameters (position of the laser focus, attenuator, number and duration of runs). Three measurements are performed and an average measurement is considered for reporting. For unstable samples, measurements are performed on supernatants. Zeta potentials are then plotted against pH to determine the stability domains and isoelectric points (IEP).

2.2. Concise results of zeta potential vs pH

2.2.1. TiO$_2$ nanomaterials

Results of zeta potential vs. pH are gathered for all TiO$_2$ NM in Figure 2.2.1. The corresponding IEP appear in the insert table. Half-filled symbols represent unstable samples which are strongly aggregated and sediment. In that case, zeta potential is measured on supernatants.
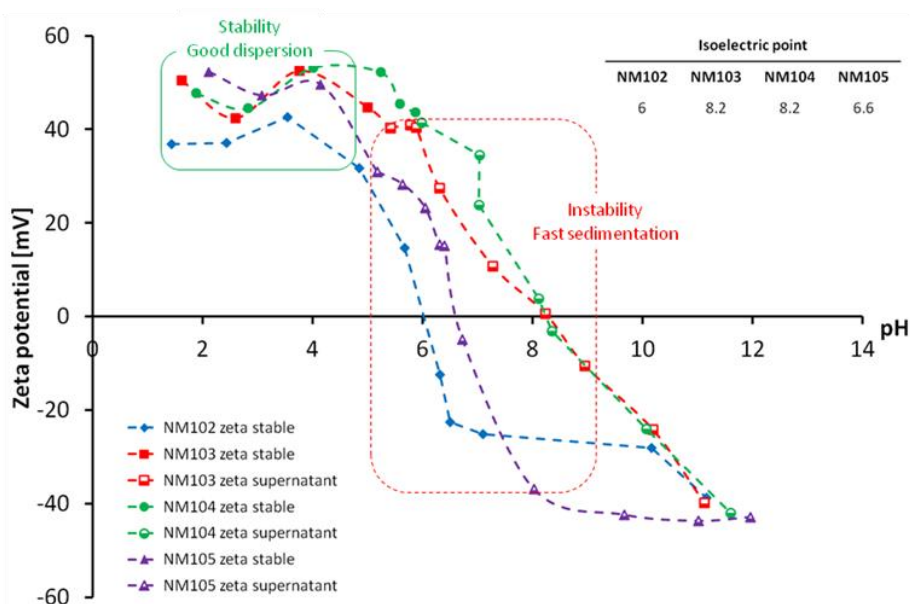
Figure 2.2.1: Zeta potential as a function of pH for TiO$_2$ NP suspensions (0.5 g/L) in constant ionic strength aqueous media (0.036 mol/L HNO$_3$/NaOH), highlighting domains of stability for acidic pH and instability around isoelectric points (values in insert). Measurements on supernatant for fast sedimenting suspensions appear as half-filled dots.

The tested TiO$_2$ NM (NM102, NM103, NM104, and NM105) form stable suspensions at acidic pH (below pH 4) where all NM have high positive charge, exceeding 30 mV. Negative zeta potentials, lower than -30 mV, were observed at high pH values (from 2 pH units above the IEP). The IEP obtained for NM102 and NM105 (pH 6 to 7), are in accordance with expected values for TiO$_2$ nanomaterials (2,3). The higher IEP of pH 8.2 observed for NM103 and NM104 can be explained by the presence of an Al$_2$O$_3$ coating on the surface of these nanoparticles (3,4). In addition, NM103 and NM104 were unstable at pH-levels around 6 despite measuring a zeta-potential of app. +40 mV on their supernatant. This may be due to surface heterogeneities of these NM.

The average aggregate sizes measured by DLS increase when increasing pH from the acidic stability domain toward the isoelectric points. This is consistent with theory where agglomeration and hence average size will increase with decreasing surface charge. For higher pH, suspensions are not stable and sediment rapidly. Stability should, however, be regained at high pH values, where the negative zeta potentials became smaller than -40 mV.

8

2.2.2. Synthetic Amorphous Silica

Results of zeta potential vs. pH are gathered for all SAS (Aynthetic Amorphous Silica) NM in Figure 2.2.2.The corresponding IEP appear in the insert table. All samples were stable and no sedimentation occurred during zeta potential measurements. The average aggregate sizes measured by DLS were roughly constant over the pH range (results not presented here).
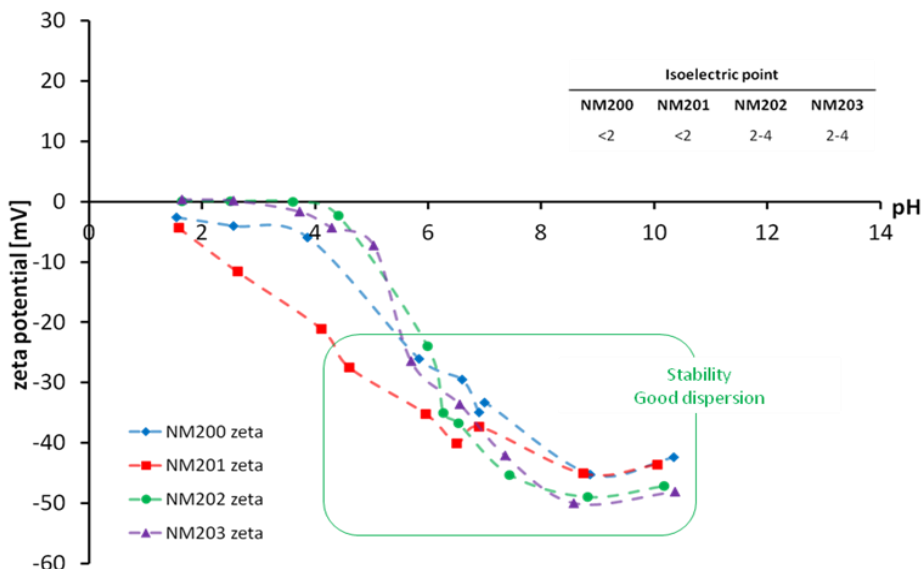
Figure 2.2.2: Zeta potential as a function of pH for SAS NM suspensions (1 g/L) in constant ionic strength aqueous media (0.036 mol/L HNO$_3$/NaOH), highlighting domains of higher stability for pH higher than 5 (isoelectric point values in insert table).

All tested silica nanomaterials form stable suspensions, with negatively to neutral charged nanoparticles. The zeta potential, however, varied greatly as function of pH and reached -40 mV around pH 7 or higher. The zeta potential variation with pH was slightly different for NM201, which is reflected in its IEP lower than 2.

3. Size distributions, mean aggregate size and structure by DLS and SAXS

Sample preparation, measurements and data treatment are only briefly reminded here but are detailed in appendix B, C and D. Results presented in this section are from the CEA only. The comparison of DLS results between partners are presented in the section 4. Detailed DLS data can be found in appendix F. All parameters used for fitting SAXS diffractograms are gathered in appendix E.

3.1. Sample preparation

The objective of this protocol is to disperse NM in the conditions giving the best dispersion state achievable in order to access the size of smallest aggregates. Suspensions are sonicated in the conditions where NM have the higher surface charge to prevent subsequent aggregation, *i.e.* in acidic conditions for TiO$_2$ NM, and in pure water (pH around 7, lowest ionic strength) for silica NM.

9

We then assume that in any other dispersion conditions (with addition of serum, BSA, buffer *etc*.), any bigger aggregate would arise from those specific conditions.

Briefly, for TiO_2 nanomaterials it consists in sonication of 3.41 mg/mL NM suspension in HNO_3 10^{-2} mol/L acidic medium at 40% amplitude for 20 min in ice-water cooling bath. For Silica nanomaterials a sonication of 6.82 mg/mL NM suspension in ultrapure water is performed also at 40% amplitude for 20 min in ice-water cooling bath. The concentrations are chosen to allow all the possible measurement in dispersion including SAXS and the preparations are presented in appendix B-III.

3.2. DLS measurements and data treatment

All measurements presented in this section were performed at CEA, following then the procedure described in appendix C for CEA. DLS measurements are performed at ambient temperature (25°C). Sample properties such as material and dispersant refractive indices and viscosity are entered in the software for analysis. Number and duration of run and optical configuration (position of laser focus and attenuation) are automatically optimized by the software for Malvern apparatus. **Three measurements** are performed and an **average measurement** is considered for reporting. The viscosity taken into account for all these measurements is the one of **pure water (0.8872 cP)**.

A monomodal model, called the cumulant analysis is used to treat the raw data correlograms (decaying as exponential). It determines a Z-average (diameter of particles scattering with higher intensity) and a polydispersity index. However, since these samples are polydisperse, more sophisticated models, such as the CONTIN method, are also applied as multimodal analysis to reveal size distributions.

DLS measurements for stability over time are performed on 500 μL suspension in semi micro polystyrene. The first measurement at t_0 is performed as usual DLS measurements. The number of run, duration, position and choice of attenuator are then recorded and used for the following measurements, which are scheduled over a period of approximatively 16 h, usually every 30 min.
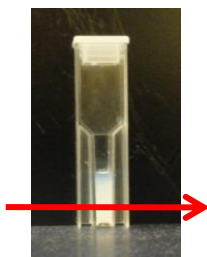
Figure 3.2.1: Semi micro cuvette used at CEA for DLS measurements at t_0 and over time. The arrow represents the position of the laser beam probing the suspension.

3.3. SAXS measurements and data treatment

SAXS measurements were performed in kapton capillaries of internal thickness 1.425 mm and run for 3600s. USAXS measurements were performed in 1 mm or 1.5 mm non-sticky double kapton cells.

Raw data, translated into intensity as a function of the scattering vector q, are first normalized by parameters of the experiments such as acquisition time, sample thickness and calibration constants determined using reference samples. The data are thus expressed in absolute scale (cm^{-1}). Backgrounds are subtracted. Once normalized and scaled, SAXS and USAXS data are concatenated.

Data from suspensions are fitted with a model describing fractal aggregates of primary particles. In this model, the whole q range is divided into sections reflecting different structural levels in the sample, and fitted by local Porod and Guinier scattering regimes. Intensity average parameters are then determined such as radius of gyration for the primaries (Rg_1) and for the aggregates (Rg_2), and a fractal dimension for the aggregates (D_f). Invariants are calculated, which give a correlation between the sample concentration and the specific surface area obtained in suspension.

3.4.   TiO$_2$ nanomaterials

3.4.1. Size distributions and intensity averaged mean size of aggregates by DLS

Intensity size distributions for one sample of each TiO$_2$ NM studied are displayed in Figure 3.4.1 (left, average measurement from 3 measurements). The corresponding number size distributions are also displayed (Figure 3.4.1, right) to illustrate the size range and proportions in number. The direct signal (correlogram of the intensity) is highly dominated by the larger particles or aggregates. Hence, when the polydispersity is large and/or big aggregates are present, the accuracy of the determination of the size of the smaller particles (even if in majority in number) is not good. The samples analyzed here are the exact same samples that were analyzed by SAXS and reported in the following paragraph.
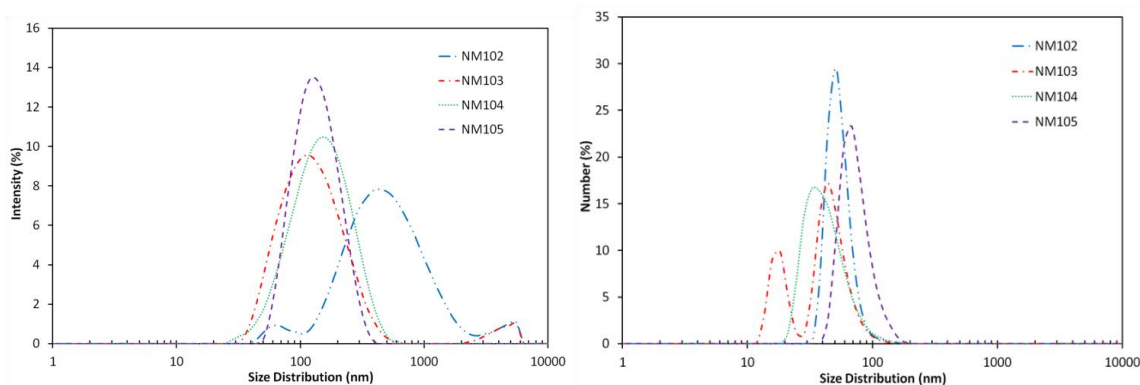
Figure 3.4.1: DLS intensity size distributions (left) and number size distributions (right) for suspensions of TiO$_2$ nanomaterials dispersed by ultrasonication (20 min - 40 % amplitude) in HNO$_3$ 10^{-2} M.

For NM103, NM104 and NM105, distributions are quite well centered at 100-150 nm with a thinner distribution for NM105. The size distribution of NM102, however, is much wider with very big aggregates of 500 nm. However, even in intensity distribution a peak of particle below 100nm is seen ; accordingly, when going to number distribution, the population of these smaller particles appears

11

to be the dominant one. Furthermore for NM102 and NM103, the presence of micron-size aggregates is revealed by the part of the fitting at long correlation times.

DLS measurements were repeated over different samples prepared independently from the same vial and from different vials to obtain mean values and standard deviation of size parameters. The results of Z-average, polydispersity index, position of the main peak in intensity size distribution and width of this peak are gathered for all TiO_2 NM in the following table.

Table 3.4.1: Size parameters and standard deviations from DLS measurements averaged on a given number of TiO_2 samples prepared by ultrasonication (20 min - 40 % amplitude) in HNO_3 10^{-2} M. Z-average, polydispersity index, position and width of the main peak in intensity size distribution.

TiO₂ nanomaterial (total number of samples)	Size parameters from DLS (intensity averaged)			
	Z-Average (nm)	PdI	Intensity distribution main peak (nm)	FWHM main peak (nm)
NM102 (7)	423.3 ± 59.4	0.427 ± 0.042	686.6 ± 40.6	414.1 ± 107.6
NM103 (6)	113.2 ± 3.2	0.242 ± 0.018	138.4 ± 7.7	73.6 ± 11.0
NM104 (5)	128.6 ± 1.3	0.221 ± 0.004	165.8 ± 5.9	89.0 ± 10.3
NM105 (6)	125.4 ± 4.2	0.171 ± 0.018	153.0 ± 5.3	69.7 ± 5.9

Over repeated samples of NM102, the mean size of aggregates in suspension is consistently much higher than for the other NM. However, the Z-average value obtained from different samples of NM102 fluctuates a lot because of the presence of micron-size aggregates. Moreover, the polydispersity index is higher than the accepted limit for analysis by the cumulant method (0.25) which indicates that such a simple monomodal description cannot be applied to accurately describe this suspension.

Concerning NM103 and NM104, even if those NM are supposed to be similar in terms of the pristine structure and size of nanoparticles, Z-average values are reproducibly found smaller for NM103 than for NM104. This could originate from the difference in their surface coating. Indeed, NM104 is registered as hydrophilic and NM103 hydrophobic. The presence of swollen hydrophilic moieties on the surface of NM104 could induce bigger hydrodynamic radii (many carboxylic acids were identified on NM104 by GC-MS). Given the relatively high polydispersities obtained, these values of Z-average and PDI can be used for comparative purposes but the size distributions are better described with multimodal analysis such as the CONTIN method, as exemplified in Figure 3.4.1.

The Z-average mean size of aggregates for NM105 is in the same range as for NM103 and NM104, however, its PDI is lower indicating a narrower size distribution.

3.4.2. Size and structure of fractal aggregates by SAXS

Experimental data from SAXS measurements on TiO_2 suspensions (exact same samples analyzed in DLS and previously reported) together with their corresponding fits by the unified model for fractal aggregates are displayed for all TiO_2 NM studied here in Figure 3.4.2.

The structure and main size parameters determined by the model, *i.e.* radius of gyration of primary particles (Rg_1), radius of gyration of aggregates (Rg_2) fractal dimension (D_f) and average number of primaries per aggregates ($N_{part/agg}$) are reported in Table 3.4.2. The full sets of parameters used for the fit of experimental curves with the unified model are gathered in appendix E.
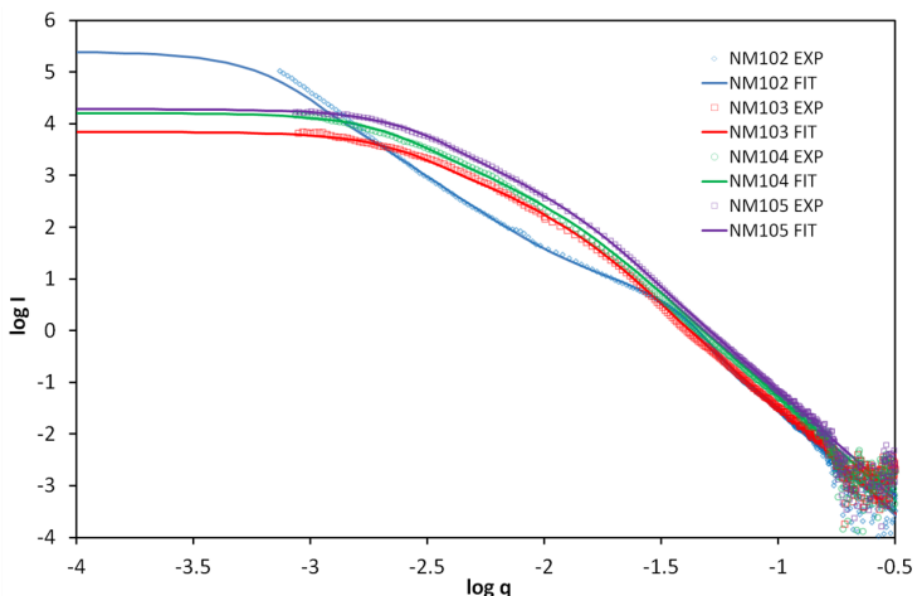
Figure 3.4.2: SAXS diffractograms fitted by the unified model for TiO_2 suspensions ultrasonicated (20 min - 40 %) in HNO_3 10^{-2} M.*NM102 cannot be perfectly fitted at low q with Df <3.

Table 3.4.2: Structure and size parameters extracted from SAXS data fitting by the unified model from TiO_2 suspensions ultrasonicated (20 min - 40 %) in HNO_3 10^{-2} M. Gyration radius of primaries and aggregates (Rg_1 and Rg_2), fractal dimension D_f and number of particles per aggregate.*NM102 cannot be perfectly fitted at low q with Df < 3.

TiO$_2$ nanomaterial	2 Rg$_1$ (nm)	2 Rg$_2$ (nm)	D$_f$	N$_{part/agg}$
NM102*	12.8	560	3	20000
NM103	26	140	2.2	113
NM104	26	160	2.3	171
NM105	26	130	2.45	117

SAXS diffractograms and the corresponding fitting size and morphology parameters unravel the differences between the four NP studied. In particular, NM102 SAXS diffractogram stands out from the other NM with a very different shape. Indeed, whereas NM103, NM104 and NM105 display very lose aggregates of fractal dimension close to 2.3, NM102 is characterized by primary particles much smaller in size (13 nm instead of 26 nm) but actually assembled into very dense and compact 3D aggregates. This is reflected in a fractal dimension of 3, even though the fit is not perfect and would

13

Co-funded by
the Health Programme
of the European Union

require an even higher D_f for best fitting (not permitted). The compacity of NM102 aggregates has been also confirmed by TEM.

Scattering signal in SAXS is sensitive to the intensity, so these values are to be correlated with intensity-based values from DLS. The mean sizes of aggregates from DLS and as determined here by SAXS are in good agreement. This SAXS model gives access to additional information on primary particle size and morphology of the aggregates.

The real concentrations of nanoparticles obtained through the invariant theorem and the specific surface areas corresponding to the Porod's plateau (data available in appendix E) were consistent with theoretical concentrations and specific surface areas of raw materials determined by SAXS on powder samples, cf. chapter on specific surface area by BET and SAXS, and midterm deliverable (1).

3.4.3. Stability over time followed by DLS

The stability of such suspensions is assessed by following in DLS the evolution of Z-average and mean count rate of resting sample over 17 h. Results for TiO_2 NM suspensions dispersed by sonication in HNO_3 10^{-2} M are reported on Figure 3.4.3.
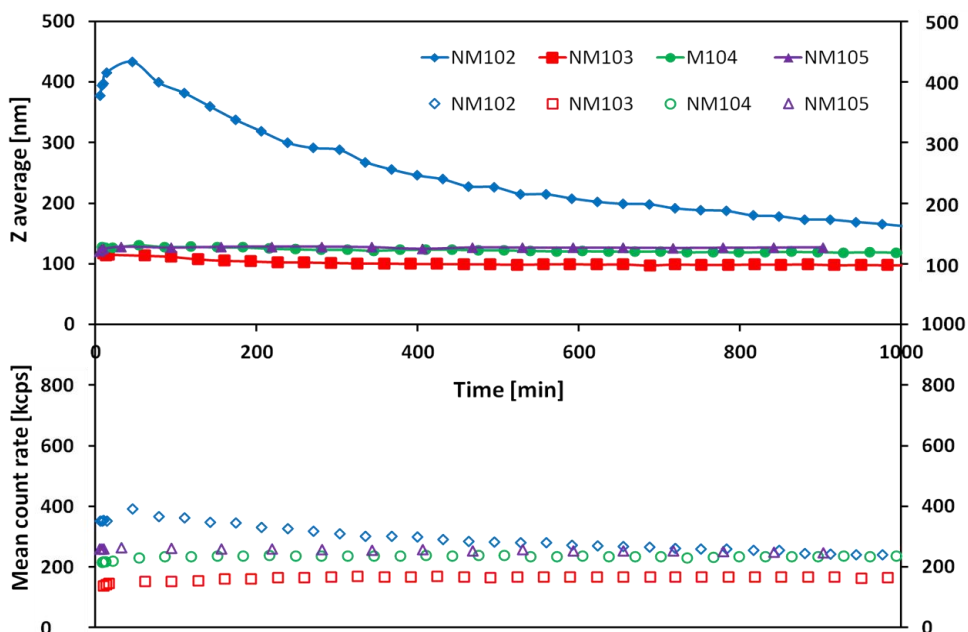
Figure 3.4.3: Evolution of DLS representative quantities (Z-average mean size, top, and mean count rate, bottom) with resting time over 17 h for TiO_2 suspensions ultrasonicated (20 min - 40 %) in HNO_3 10^{-2} M.

For NM103, NM104 and NM105, the mean count rate (mainly proportional to the concentration at the position of the laser beam) and Z-average stay stationary unraveling that almost no sedimentation occurs and the suspensions are very stable.

14

On the other hand, a sedimentation trend is observed for NM102. Indeed, even in the best dispersion conditions the aggregates in suspensions are much bigger (400 – 600 nm) than for the 3 other NM. The slow sedimentation of the biggest aggregates, induced by gravity, gives rise to a regular decrease of Z-average mean size measured at the position of the laser beam, while the mean count rate is less affected.

3.5. Synthetic Amorphous Silica

3.5.1. Size distributions and intensity averaged mean size of aggregates by DLS

Intensity size distributions for samples of silica NM studied are displayed in Figure 3.5.1 (left, averaged on 3 measurements). The corresponding number size distributions are also displayed (Figure 3.5.1, right) to illustrate the size range and proportions in number. However, as mentioned for TiO_2 NM, the high polydispersity and the presence of big aggregates, results in an intensity signal highly dominated by the bigger aggregates and a very poor accuracy on the size determined for smaller particles. The samples displayed here are the exact same samples that are analyzed by SAXS in the following paragraph.
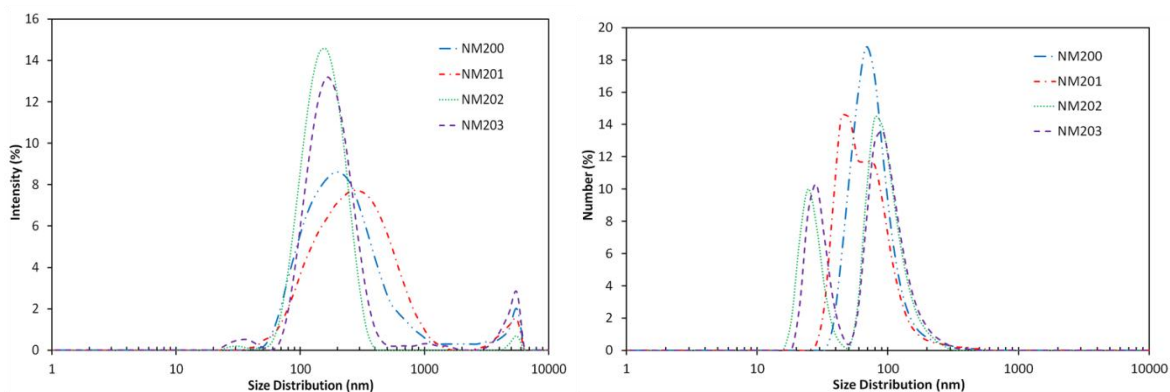
Figure 3.5.1: DLS intensity size distributions (left) and number size distributions (right) for suspensions of silica nanomaterials dispersed by ultrasonication (20 min - 40 % amplitude) in ultrapure water.

Intensity size distributions are very broad and reveal the presence of very big aggregates of a few microns. The dispersion conditions used for sample preparation might not be optimal (this higher concentration of 6.82 g/L chosen for SAXS measurement is maybe too high for light scattering). NM202 and NM203 display size distributions thinner and centered around slightly smaller values than NM200 and NM201.

DLS measurements were repeated over different samples prepared from the same vial and from different vials to obtain mean values and standard deviation of size parameters. The results of Z-average, polydispersity index, position of the main peak in intensity size distribution and width of this peak are gathered for all silica NM in the following table.

The previous observations are confirmed. However, polydispersity indices are all higher than 0.25 which indicates that such a monomodal description is not suitable to describe the suspensions accurately. These values can be used for comparative purposes (in the next section on vial homogeneity) but the real size distributions are only well described by multimodal analysis such as displayed in Figure 3.5.1.

Table 3.5.1: Size parameters and standard deviations from DLS measurements averaged on a given number of silica samples prepared by ultrasonication (20 min - 40 % amplitude) in ultrapure water. Z-average, polydispersity index, position and width of the main peak in intensity size distribution.

Silica nanomaterial (total number of samples)	Size parameters from DLS (intensity averaged)			
	Z-Average (nm)	PdI	Intensity distribution main peak (nm)	FWHM main peak (nm)
NM200 (5)	207.8 ± 11.9	0.388± 0.036	234.9 ± 18.6	160.4 ± 43.4
NM201 (3)	200.7 ± 27.6	0.342 ± 0.026	224.2 ± 79.0	117.2 ± 84.9
NM202 (2)	175.9 ± 4.5	0.355 ± 0.001	159.9 ± 1.8	56.2 ± 2.9
NM203 (3)	175.0 ± 7.4	0.409 ± 0.035	172.1 ± 15.5	76.3 ± 13.4

3.5.2. Size and structure of fractal aggregates by SAXS

Experimental data from SAXS measurements on silica suspensions (exact same samples analyzed in DLS and previously reported) together with their corresponding fits by the unified model for fractal aggregates are displayed in Figure 3.5.2.

The structure and main size parameters determined by the model, *i.e.* radius of gyration of primary particles (Rg_1), radius of gyration of aggregates (Rg_2) fractal dimension (D_f) and average number of primaries per aggregates ($N_{part/agg}$) are reported in Table 3.5.2. The full sets of parameters used for the fit of experimental curves with the unified model are gathered in appendix E.

Table 3.5.2: Structure and size parameters extracted from SAXS data fitting by the unified model from Silica suspensions ultrasonicated (20 min - 40 %) in pure water. Gyration radius of primaries and aggregates (Rg_1 and Rg_2), fractal dimension D_f and number of particles per aggregate.*NM203 cannot be fitted at low q with correct parameters and very different values would lead to the same (bad) quality of fit.

Silica nanomaterial	Main size and structure parameters from SAXS unified fit model			
	2 Rg_1 (nm)	2 Rg_2 (nm)	D_f	$N_{part/agg}$
NM200	18	440	2.45	3600
NM201	20	180	2.45	457
NM202	16	100	2.5	200
NM203*	-	-	-	-
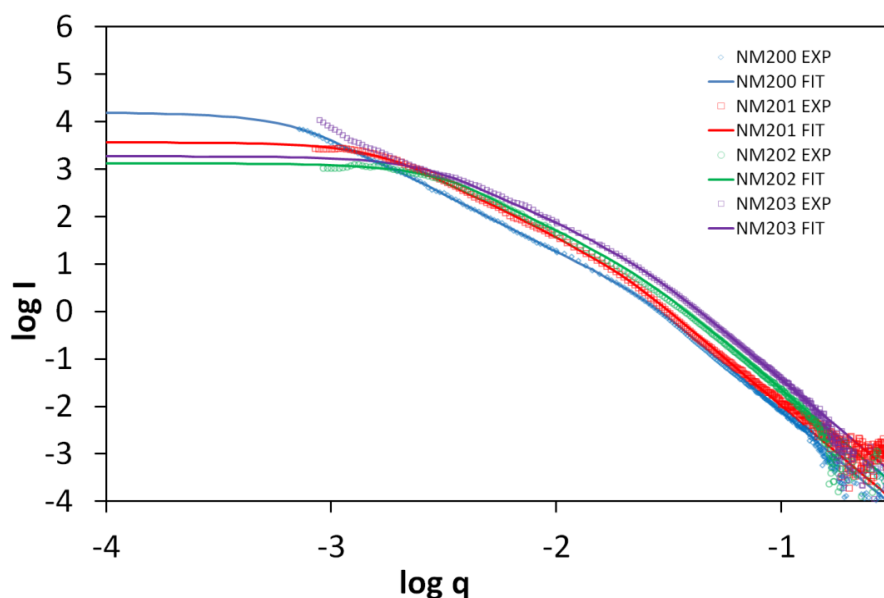
Figure 3.5.2: SAXS diffractograms fitted by the unified model for Silica suspensions ultrasonicated (20 min - 40 %) in pure water.*NM203 cannot perfectly fitted at low q with correct parameters.

The upturn of intensity observed at low q for NM203 cannot be fitted by the model. Therefore, the parameters extracted from such a poor quality fit are not reliable and therefore not reported here. The tested silica NM exhibit roughly the same fractal structure, with slight differences in primary particle size and aggregate size. NM202 display smaller aggregate size than NM201 and NM200.

The real concentrations of nanoparticles obtained through the invariant theorem and the specific surface areas corresponding to the Porod's plateau were consistent with theoretical concentrations and specific surface areas of raw materials determined by SAXS on powder samples, cf. chapter on specific surface area by BET and SAXS, and midterm deliverable (1).

3.5.3. Stability over time followed by DLS

The stability of silica suspensions was tested following in DLS the evolution of Z-average and mean count rate over 17 h. Results are reported on Figure 3.5.3.

In general for all the synthetic amorphous silica NM studied, a slight sedimentation is observed during the first hour and then the samples are very stable for the next 16 h (stationary state of Z-average and mean count rate).
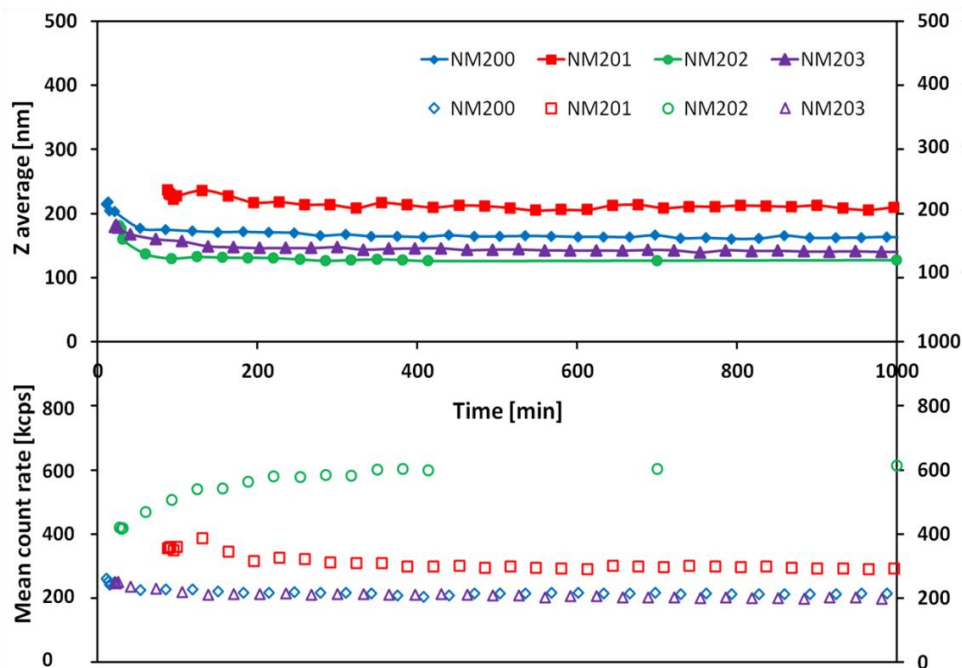
Figure 3.5.3: Evolution of DLS representative quantities (Z-average mean size, top, and mean count rate, bottom) with resting time over 17 h for Silica suspensions ultrasonicated (20 min - 40 %) in pure water.

4. Homogeneity of sub-sampling into vials and reproducibility of sample preparation among partners

4.1. Procedure

The repeatability of the sample preparation using of sub-samples taken from specific NM vials provided by the JRC, was assessed by DLS measurements on aqueous suspensions in the pH-optimized dispersion states identified in Chapter 2. The same sample preparation protocol was applied by all partners (CEA, INRS, NRCWE), as described in previous section and appendix B. Beyond

18

sub-sample and vial-to-vial inhomogeneity, the main technical difference leading to variability in the dispersions could arise from the use of different sonicators (see appendix C). The comparison of measurements and data treatment procedures between the different DLS apparatus, *i.e.* Zetasizer NanoZS from Malvern Instrument for CEA and NRCWE, and Vasco Cordouan for INRS is discussed in appendix C. The main analysis was made suing NM104, NM105, NM200 and NM203. However additional data on other NM are also reported when available.

In a first stage, the homogeneity of a given vial is assessed by DLS measurements performed on a series of samples prepared by the same operator, in the same conditions and from the same vial number. These comparisons actually illustrate both the homogeneity inside one vial and the reproducibility of the sample preparation from a given operator.

Moreover, a series of samples prepared by the different partners from different vial numbers of a given NM were also measured to quantify both the variability between vials of the same NM, and between sample preparations from the different partners.

The main results are reported below for each nanomaterial, comparing either samples from the same vial or samples from different vials. When several samples were run on one vial number, mean values with standard deviations are reported. The data reported are Z-average and polydispersity index, calculated using the cumulant method both for Malvern and Vasco Cordouan apparatus, and the position of the main peak of the intensity size distribution modeled with a multimodal analysis. For Malvern apparatus, the CONTIN method is used and the width (FWHM) of this main peak is also reported. For Cordouan apparatus, this peak corresponds to the position of the main mode obtained with the Padé-Laplace method.

The complete sets of data are available in the appendix F.

4.2. TiO$_2$ nanomaterials

4.2.1. NM102

Results for repeated samples of NM102 suspensions from the same vial are reported in Table 4.2.1, in order to estimate the reproducibility of sample preparation and intra-vial homogeneity. Results obtained from different vial numbers and different partners are gathered in Table 4.2.2 for estimation of homogeneity between vials and variability between partners.

NM102 samples exhibit a poor reproducibility of about 20%. Nevertheless, as mentioned in the previous section, these suspensions contain very big aggregates of micron-size exhibit a high polydispersivity and are prone to sedimentation. Therefore, the variability observed more likely comes from inappropriate DLS data treatment method than from any problem of homogeneity of sub-sampling. Furthermore, the intra-vial variability is actually higher than the one observed between different vials, so no conclusion can be drawn and the vials are assumed to be homogeneous.

Table 4.2.1: DLS main size parameters (Z-average, polydispersity index, position of the main peak in intensity distribution and width of this peak) obtained from independent suspensions of NM102 prepared from the same vial in the same conditions but at different dates.

NM10X	partner	vial n°	repetition /date	Z-Average	PdI	Intensity distribution main peak	FWHM main peak
NM102	CEA	34	20110719	533.3	0.486	964.5	796.3
			20110802	377.9	0.419	587.4	417.3
			20110729	380.3	0.352	622.5	362.8
			20111006	478.8	0.455	633.6	264.7
intra vial				**442.6+/-76.6**	**0.428+/- 0.058**	**702.0+/- 176.1**	**460.3 +/- 232.7**

Table 4.2.2: DLS main size parameters (Z-average, polydispersity index, position of the main peak in intensity distribution and width of this peak) obtained from independent suspensions of NM102 prepared from different vial numbers.

NM10X	partner	vial n°	Z-Average	PdI	Intensity distribution main peak	FWHM main peak
NM102	CEA	34 (4)	442.6 +/-76.6	0.428 +/- 0.058	702.0 +/- 176.1	460.3 +/- 232.7
NM102	CEA	35	403.1	0.411	695.8	373.9
NM102	CEA	24	400.4	0.441	654.8	493.2
NM102	CEA	31	389.5	0.426	685.4	572.4
Average over the 4 vials			**408.9 (+/-23.2)**	**0.427 (+/-0.012)**	**684.5 (+/-21.0)**	**474.9 (+/-82.2)**

4.2.2. NM103

Results for repeated samples of NM103 suspensions from the same vial for each partner and from different vial numbers between the partners are reported in Table 4.2.3.

Table 4.2.3: DLS main size parameters (Z-average, polydispersity index, position of the main peak in intensity distribution and width of this peak) obtained from independent suspensions of NM103 prepared from the same vial in the same conditions.

NM10X	partner	vial n°	repetition /date	Z-Average	PdI	Intensity distribution main peak	FWHM main peak
NM103	CEA	47	20100927	112.1	0.244	139.2	72.3
			20110718	115.7	0.253	137.9	69.3
			20110722	113.6	0.258	139.5	80.3
	intra vial			113.8+/-1.8	0.252+/- 0.007	138.9+/- 0.9	74.0 +/- 5.7
NM103	CEA	557	20110729	117.3	0.212	148	78.1
			20110915	112.6	0.255	141.4	86.5
			20110930	108	0.229	124.5	54.8
	intra vial			112.6+/-4.7	0.232+/- 0.022	138.0+/- 12.1	73.1 +/- 16.4
NM103	INRS	576	N1	138.7	0.244	123.1	
			N2	133.7	0.202	117.5	
			N3	124.4	0.115	117.5	
	intra vial			132.3+/-7.3	0.187+/- 0.066	119.4+/- 3.2	
	Average over the 3 vials			119.6+/-11.0	0.224+/-0.33	132.1+/-11.0	

The reproducibility intra vial is of a few percents for each partner, which demonstrates a rather good homogeneity of each vial of NM103, and a good reproducibility of the sample preparation by each partner.

The reproducibility inter vial for the 2 vials tested at CEA is of a few percent also. However, a systematic variation (15%) from one partner to the other is observed, which is beyond the intravial reproducibility. This variability is thought to originate from systematic deviation between partners, especially because of the different types of sonicator used for dispersion, and not from inhomogeneities between vial numbers.

4.2.3. NM104

Results for repeated samples of NM104 suspensions from the same vial are reported in Table 4.2.4 and values obtained from different vial numbers and different partners are gathered in Table 4.2.5.

Table 4.2.4: DLS main size parameters (Z-average, polydispersity index, position of the main peak in intensity distribution and width of this peak) obtained from independent suspensions of NM104 prepared from the same vial in the same conditions.

NM10X	partner	vial n°	repetition /date	Z-Average	PdI	Intensity distribution main peak	FWHM main peak
NM104	CEA	465	20110722	130.6	0.226	169	91.0
			20110907	127.1	0.218	164.8	87.5
			20110929	129	0.216	156.7	74.7
intra vial				**128.9+/-1.8**	**0.220+/- 0.005**	**163.5+/- 6.3**	**84.4 +/- 8.6**
NM104	NRCWE	1157	1	125.9	0.220	161.8	85.4
			2	125.4	0.201	159.4	81.1
			3	123.5	0.196	155.0	74.6
			4	127.9	0.220	167.2	89.4
			5	124.0	0.211	158.7	83.0
intra vial				**125.3+/-1.7**	**0.210+/- 0.011**	**160.4+/- 4.5**	**82.7 +/- 5.5**

Table 4.2.5: DLS main size parameters (Z-average, polydispersity index, position of the main peak in intensity distribution and width of this peak) obtained from independent suspensions of NM104 prepared from different vial numbers.

NM10X	partner	vial n°	Z-Average	PdI	Intensity distribution main peak	FWHM main peak
NM104	CEA	39 (2)	128.3 +/- 0.8	0.222 +/- 0.003	169.2 +/- 4.5	95.9 +/- 10.9
NM104	CEA	465 (3)	128.9 +/-1.8	0.220 +/- 0.005	163.5 +/- 6.3	84.4 +/- 8.6
NM104	NRCWE	1157 (5)	125.3 +/- 1.7	0.210 +/- 0.011	160.4 +/- 4.5	82.7 +/- 5.5
NM104	NRCWE	803	124.6	0.204	160.0	80.1
NM104	NRCWE	885	129.6	0.229	166.9	91.2
Average 3 vials NRCWE			**126.5 +/-2.7**	**0.214 +/-0.013**	**162.4 (+/-3.9)**	**84.7 (+/-5.8)**
Average over the 5 vials			**127.3+/-2.2**	**0.217+/-0.010**	**164.0+/-4.0**	**86.9+/-6.5**

The reproducibility intra vial is of a few percents for each partner, which demonstrates a very good homogeneity of each vial of NM104, and a good reproducibility of the sample preparation by each partner.

The reproducibility inter vial for the 3 vials tested at NRCWE is of a few percent also. The same order is observed when comparing vials from both partners. Hence, the homogeneity intra-vial and inter-vial for NM104 are both of the same order and very good.

4.2.4. NM105

Results for repeated samples of NM105 suspensions from the same vial are reported in Table 4.2.6Table 4.2.1, and values obtained from different vial numbers and different partners are gathered in Table 4.2.7.

Table 4.2.6: DLS main size parameters (Z-average, polydispersity index, position of the main peak in intensity distribution and width of this peak) obtained from independent suspensions of NM105 prepared from the same vial in the same conditions.

NM10X	partner	vial n°	repetition /date	Z-Average	PdI	Intensity distribution main peak	FWHM main peak
			20100209	128	0.162	155.1	69.7
			20101006	120.7	0.192	152.4	74.7
NM105	CEA	305	20101011	121.6	0.189	153.3	73.7
			20110705	122.7	0.143	143.1	58.4
			20110928	129.3	0.172	156.2	69.6
	intra vial			124.5 +/-3.9	0.172 +/- 0.020	152.0 +/- 5.2	69.2 +/- 6.5

Table 4.2.7: DLS main size parameters (Z-average, polydispersity index, position of the main peak in intensity distribution and width of this peak) obtained from independent suspensions of NM105 prepared from different vial numbers.

NM10X	partner	vial n°	Z-Average	PdI	Intensity distribution main peak	FWHM main peak
NM105	CEA	305 (5)	124.5 +/-3.9	0.172 +/- 0.020	152.0 +/-5.2	69.2 +/- 6.5
NM105	CEA	2176	130.1	0.170	158.1	72.3
NM105	INRS	2194 (2)	132.9 +/-1.6	0.057 +/- 0.006	138.1 +/-4.5	
NM105	NRCWE	2758	135.6	0.134	156.5	61.8
NM105	NRCWE	2749	127.9	0.145	151.4	63.9
NM105	NRCWE	2701	127.8	0.143	150.7	61.9
Average 3 vials NRCWE			130.4 +/-4.5	0.141 (+/-0.006)	152.9 (+/-3.2)	62.5 (+/-1.2)
Average over the 6 vials			129.8+/-4.0	0.137+/-0.042	151.1+/-7.0	

The reproducibility intra-vial performed at CEA is of a few percents, which demonstrates a rather good homogeneity of each vial of NM105, and a good reproducibility of the sample preparation.

The reproducibility inter vial for the 3 vials tested at NRCWE is of a few percent also. Except for the polydispersity index which is found much lower at INRS, the same order of data is observed when comparing the six vials from the three partners. Hence, the homogeneity intra-vial and inter-vial for NM105 are both of the same order and good.

From the data obtained by all partner, the polydispersity of NM105 is the lowest of the different TiO$_2$ materials tested.

4.3. Synthetic Amorphous Silica

4.3.1. NM200

Results for repeated samples of NM200 suspensions from the same vial are reported in Table 4.3.1, and values obtained from different vial numbers and different partners are gathered in Table 4.3.2.

The reproducibility intra-vial seems very dependent on the measurand. At INRS, the variability of data from the cumulant analysis (Z-average and PdI) is only of a few percents, whereas it is much higher for the position of the peak obtained from Padé-Laplace analysis. At CEA, the variability intra-vial observed is about 6-10 %.

Table 4.3.1: DLS main size parameters (Z-average, polydispersity index, position of the main peak in intensity distribution and width of this peak) obtained from independent suspensions of NM200 prepared from the same vial in the same conditions.

NM20X	partner	vial n°	repetition /date	Z-Average	PdI	Intensity distribution main peak	FWHM main peak
NM200	INRS	109	N1	238.5	0.246	338.9	
			N2	243.0	0.244	281.9	
			N3	240.0	0.255	257.1	
	intra vial			**240.5+/-2.3**	**0.248+/- 0.006**	**292.7+/- 42.0**	
NM200	CEA	50	20101005	222	0.435	244.4	158.8
			20110202	198.5	0.371	218.1	115.3
			20110922	195.6	0.343	226.7	134.9
			20111116	212.4	0.412	262.9	230
	intra vial			**207.1+/-12.3**	**0.390+/- 0.041**	**238.0+/- 19.9**	**159.8 +/- 50.1**

Table 4.3.2: DLS main size parameters (Z-average, polydispersity index, position of the main peak in intensity distribution and width of this peak) obtained from independent suspensions of NM200 prepared from different vial numbers.

NM20X	partner	vial n°	Z-Average	PdI	Intensity distribution main peak	FWHM main peak
NM200	CEA	50 (4)	207.1 +/-12.3	0.390 +/- 0.041	238.0 +/-19.9	159.8 +/- 50.1
NM200	CEA	95	195.3	0.378	222.4	163.1
NM200	INRS	109 (3)	240.5 +/-2.3	0.248 +/- 0.006	292.7 +/-42.0	
NM200	NRCWE	279	183.2	0.244	215.0	109.6
NM200	NRCWE	494	184.8	0.237	226.3	125.8
NM200	NRCWE	372	176.6	0.232	215.9	114.6
Average 3 vials NRCWE			**181.5 (+/-4.3)**	**0.238 (+/-0.006)**	**219.1 (+/-6.3)**	**116.7 (+/-8.3)**
Average over the 6 vials			**197.9+/-23.4**	**0.288+/-0.075**	**235.0+/-29.4**	

When comparing the 3 vials tested at NRCWE, the inter vial homogeneity seems very good (2-3%) even better than the intra-vial homogeneity observed at CEA. However, the size order of NM200 obtained by each partner is quite different, so when comparing the 6 vials from the 3 partners, the variability is higher than 10%. Given the consistency of the results obtained from each partner, the vials are thought to be rather homogeneous and the variations may originate from a systematic difference of sample preparation caused by the different types of sonicator, when applied to NM200 suspensions.

4.3.2. NM203

Results for repeated samples of NM203 suspensions from the same vial are reported in Table 4.3.3. Table 4.2.1, and values obtained from different vial numbers and different partners are gathered in Table 4.3.2.

Table 4.3.3: DLS main size parameters (Z-average, polydispersity index, position of the main peak in intensity distribution and width of this peak) obtained from independent suspensions of NM203 prepared from the same vial in the same conditions

NM20X	partner	vial n°	repetition /date	Z-Average	PdI	Intensity distribution main peak	FWHM main peak
NM203	INRS	227	N1	218.9	0.290	141.3	
			N2	288.2	0.327	154.9	
			N3	230.1	0.281	148.0	
	intra vial			**245.7+/-37.2**	**0.299+/- 0.024**	**148.1+/- 6.8**	
NM203	NRCWE	169	1	142.2	0.219	169.7	77.5
			2	149.9	0.247	189.6	99.1
			3	152.4	0.259	181.3	84.7
			4	145.6	0.250	171.6	76.5
	intra vial			**147.5+/-4.5**	**0.244+/- 0.017**	**178.1+/- 9.2**	**84.4 +/- 10.4**

As for NM200, the size order obtained or NM203 from the three partners are relatively different. Therefore the variability between the 6 vials tested by the 3 partners is quite high (20%). However, the reproducibility intra-vial obtained from CEA and from INRS are reasonable (a few to ten percent). The variability inter-vial from the three vials tested at NRCWE is even lower than the intra-vial variability. Therefore, the vials are considered rather homogeneous and the variations observed may originate from a systematic difference of sample preparation caused by the different types of sonicator, when applied to NM203 suspensions.

Table 4.3.4: DLS main size parameters (Z-average, polydispersity index, position of the main peak in intensity distribution and width of this peak) obtained from independent suspensions of NM203 prepared from different vial numbers.

NM20X	partner	vial n°	Z-Average	PdI	Intensity distribution main peak	FWHM main peak
NM203	CEA	207 (2)	172.9 +/-9.2	0.427 +/- 0.025	181.0 +/-4.0	82.5 +/- 11.3
NM203	CEA	118	179.2	0.375	154.5	63.9
NM203	INRS	227 (3)	245.7 +/-37.2	0.299 +/- 0.024	148.1 +/-6.8	
NM203	NRCWE	169 (4)	147.5 +/-4.5	0.244 +/-0.017	178.1 +/-9.2	84.4 +/-10.4
NM203	NRCWE	294	146.3	0.214	183.1	83.6
NM203	NRCWE	212	146.6	0.229	181.7	83.4
Average 3 vials NRCWE			**146.8 (+/-0.6)**	**0.229 (+/-0.015)**	**181.0 (+/-2.6)**	**83.8 (+/-0.6)**
Average over the 6 vials			**173.0 +/-38.4**	**0.298 +/-0.086**	**171.1 +/-15.5**	

5. *Summary and conclusions*

The sizes measured by DLS are corresponding to the one of the aggregates of primary particles. On the other hand SAXS can measure both the aggregates size and the primary size of the particles. The agreement is good for TiO_2 nanomaterials and very good for silica except for NM203 for which SAXS failed to obtain the size of the aggregates (out of range) using the proposed model. DLS being correct for this nanomaterial, this means that the geometry of the aggregates of primary is more complex than the one proposed.

All the obtained suspensions but NM102 are stable at least during 16hours.

Regarding homogeneity, using DLS and comparison between measurements on different vials in different institute from this consortium it concluded that the vials of titania and silica can be considered rather homogeneous and the variations observed may originate from a systematic difference of sample preparation caused by the different types of sonicator, when applied to NM203 suspensions.

Co-funded by
the Health Programme
of the European Union

References

This report is based on the interim project reports and direct contributions from all co-authors. All internal documents are available on CIRCABC for NANOGENOTOX consortium members.

1. Guiot, C.; Spalla, O.; de Temmeman, P-J.; Mast, J.; Shivachev, B.; Birkedal, R.; Levin, M.; Nielsen, S.H.; Koponen, I.K.; Clausen, P.A.; Jensen, K.A.; Rousset, D.; Bau, S.; Bianci, B.; Witschger, O.; Motzkus, C.; *Nanomaterial datasets with requested physicochemical properties – Midterm Deliverable, Key intrinsic physicochemical characteristics of NANOGENOTOX nanomaterials.* KA Jensen and N Thieret (Eds.): August 2011; 44 pp.
2. Mandzy, N.; Grulke, E.; Druffel, T., *Breakage of TiO$_2$ agglomerates in electrostatically stabilized aqueous dispersions.* Powder Technol. 2005, 160 (2), 121-126.
3. Marek, K., *Compilation of PZC and IEP of sparingly soluble metal oxides and hydroxides from literature*. Adv. Colloid Interface Sci. 2009, 152 (1-2), 14-25.
4. Singh, B. P.; Menchavez, R.; Takai, C.; Fuji, M.; Takahashi, M., *Stability of dispersions of colloidal alumina particles in aqueous suspensions.* J. Colloid Interface Sci. 2005, 291 (1), 181-186.

Appendix A : Standard Operating Procedure for Surface charge and isoelectrical point of TiO₂ and Silica by zetametry

Camille Guiot and Olivier Spalla (CEA)

I. General description

Dispersion state and stability of suspensions are governed by an equilibrium between attractive (mainly van der Waals) and repulsive (electrostatic or steric) interactions. A stable suspension is obtained if the repulsive interactions overcome the attractive ones, responsible for aggregation and subsequent sedimentation. Zeta potential is a good index of the magnitude of repulsive interactions between charged particles. The charge at the very surface of the particles is not accessible. Zeta potential corresponds actually to the potential at the shear plane; i.e. the boundary between the bulk dispersant and the double layer of solvent and ions moving together with the particles (outer limit of Gouy-Chapman layer (Fig. A1). κ^{-1}, called the reciprocal Debye length, represents the thickness of this double layer. This zeta-potential varies with pH due to protonation-deprotonation of the material surface. From colloid science, a suspension of small particles is considered stable if the zeta-potential exceed |30| mV.
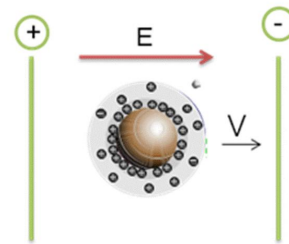
In acidic medium, the surface of metal oxide materials is protonated (MOH_2^+) leading to positively charged particles, whereas for high pH the deprotonation results in negatively charged particles (MO^-). The pH-value where the charge is reversed determines the so-called isoelectric point (IEP) at which the dispersion is unstable (screening of stabilizing electrostatic interactions). The IEP can be determined by titration, but can also be measured from different dispersions prepared manually and displaying the same ionic strength for various pH. The zeta potential can be greatly influenced by the properties of the medium, such as ionic strength (by compression of the double layer), or adsorbing molecules or ions (especially multivalent ions)

The zeta potential (ζ) is calculated from the measurement of electrophoretic mobility U_E using Henry's equation:

$$U_E = \frac{2\,\varepsilon\,\zeta\,f(\kappa a)}{3\eta}$$

ε: dielectric constant of medium
η: viscosity
κ: inverse of the Debye length, a: radius of a particle
$f(\kappa a)$ = 1.5 for aqueous suspensions in the Smoluchowski approximation

In practice, the sample is submitted to an electric field which induces the movement of charged particles towards the opposite electrode.

I

II. Chemicals and equipment

- HNO$_3$ (analytical grade)
- NaOH (analytical grade)
- NaNO$_3$ (analytical grade)
- Purified water (MilliQ or Nanopure water)
- The US apparatus can be a Ultrasonic probe Sonics & Materials, VCX500-220V, 500 W, 20 kHz equipped with a standard 13 mm disruptor horn, or equivalent.
- pH-meter can be the Nano ZS (e.g, Malvern Instruments), equipped with laser 633 nm
- Autotitrator (Malvern MPT-2) –*optional for automatic determination of IEP*
- Malvern software (DTS 5.03 or higher) installed on a computer to control the Zetasizer
- Using the Malvern instrument the clear disposable zeta cells can be DTS1061 - DTS1060C

III. Sample preparation

Brief

Samples for zeta potential measurements are prepared as aqueous suspensions of 0.5 g/L for TiO$_2$ nanomaterials, and 1 g/L for Silica nanomaterials with constant ionic strength of 0.036 mol/L (monovalent salt) and controlled pH. They are prepared by dilution of concentrated sonicated stock suspensions of 10 g/L into pH and ionic strength controlled "buffers" prepared by addition of HNO$_3$, NaOH and NaNO$_3$ in various proportions.

Stock suspension preparation

20 mL of stock suspensions of 10 g/L NM (Silica or TiO$_2$) in pure water are prepared using the following steps:

- 200 mg of NM are weighed and introduced in a 20 mL gauged vial (with protective gloves, mask and glasses, and damp paper towel around the weigh-scale).
- The 20 mL gauged vial is completed with ultrapure water (MilliQ)
- The suspension is transferred into a flask suitable for sonication (here a 40 mL large-neck glass flask of internal diameter 38 mm was used, height of 20 mL liquid 20 mm), making sure that all the settling material is recovered.
- The suspension is dispersed by ultrasonication for 20 min at 40% in an ice-water bath. Probe, sample and bath are placed in a sound abating enclosure, and inside a fume hood.

Preparation of "buffer" solution

Denominated *"buffer"* solutions are aqueous ionic solutions of Na$^+$, H$^+$, NO$_3^-$ and OH$^-$, designed to display the same ionic strength with a modulated pH.

- A first set of concentrated buffer solutions (0.1 mol/L of salt, various pH) are prepared by addition of HNO$_3$, NaOH and NaNO$_3$ in various proportions in ultrapure water.

- Then, 20 mL of these concentrated buffers are poured into 50 mL gauged vials completed with ultrapure water, to lead to a new set of buffers with a salt concentration of 0.04 mol/L and a pH ranging from 1.5 to 12.5. The combination of two consecutive buffers gives access to the necessary intermediate pH.
- By this procedure, acidic buffers contain 0.04 mol/L of NO_3^- and various ratios of Na^+/H^+ as counter ions; likewise, basic buffers contain 0.04 mol/L of Na^+ and various ratios of NO_3^-/OH^-.

Preparations of suspensions for zeta potential measurements and determination of isoelectric point

In this SOP Zeta potential measurements are performed on:

- 0.5 g/L suspensions for TiO_2 samples
- 1 g/L suspensions for Silica sample (the lower refraction index of Silica requires higher concentration).

For TiO_2 samples, freshly sonicated stock suspensions are first two-fold diluted in ultrapure water to get 5 g/L concentrated suspensions. For Silica samples, 10 g/L suspensions are used right after sonication.

Series of samples are prepared by addition of 400 µL of concentrated NM suspension (10 g/L for Silica and 5 g/L for TiO_2) and 3.6 mL of 0.04 mol/L buffer solutions in a 5 mL glass flask. This lead to samples of 0.5 g/L TiO_2 or 1 g/L Silica and a constant ionic concentration of 0.036 mol/L in monovalent salt.

For each NM, an additional sample is prepared in MilliQ or Nanopure water with the same NM concentrations, *i.e.* by addition of 400 µL of concentrated NM suspension and 3.6 mL of water.

IV. *Measurements and data treatment*

Brief

> **For each suspension of known pH, fixed ionic strength and fixed NM concentration, zeta potential is measured on a general purpose mode with automatic determination of measurement parameters. Three measurements are performed and averaged for reporting. For unstable samples, measurements are performed on supernatants. Zeta potentials are then plotted against pH to determine the stability domains and isoelectric points (IEP).**

Measurements

Equilibrium pH of the suspensions are measured and considered as pH data for the reported results.

Suspension characterized by zetametry are inserted in Malvern patented folded capillary cells with gold electrodes (volume 0.75 to 1 mL), DTS1061. Zeta measurements are performed on the "*general purpose*" mode at 25°C with automatic optimization of laser power, voltage settings, the number of runs (10 - 100) and run duration. The analysis is repeated 3 times with no equilibration time (sample already at ambient temperature).

III

The Smoluchowski model (F(κa)=1.5) was used, considered the high polarity of aqueous solvent, and hence a thin double layer around the particles. For the dispersant, the refractive index R_i, absorption R_{abs}, viscosity and di-electric properties considered are the one of pure water. The parameters used for dispersant and material properties are listed in the following table.

Table A.1. : Properties of dispersant and material phases used for zeta potential measurements

	Water (STP)	TiO$_2$	silica$_{(amorphous)}$
R_i	1.33	2.49	1.5
R_{abs}		0.01	0.01
Viscosity [cP]	0.8872	-	-

Data treatment

Electrophoretic mobility is measured by a combination of laser Doppler velocimetry, a technique based on the phase shift of the laser beam induced by the movement of particles under an electric field, and phase analysis light scattering (patented M3-PALS technique). In this "mixed mode measurement" (M3), the measurement consists in the application of an alternative electric field in two modes, a fast field reversal mode, and a slow field reversal mode. The light scattered at an angle 17° is combined with the reference beam and the resulting signal is treated by the computer (Figure A.2). During the fast field reversal mode, the electro-osmose effect is negligible, allowing to determine an accurate mean zeta potential, whereas the slow field reversal mode helps modeling the distribution of potentials. An example of the main data plots returned by DTS software from zeta potential measurements is shown on figure A.3 (phase plot and corresponding electric field applied, mean zeta potential and zeta potential distribution).
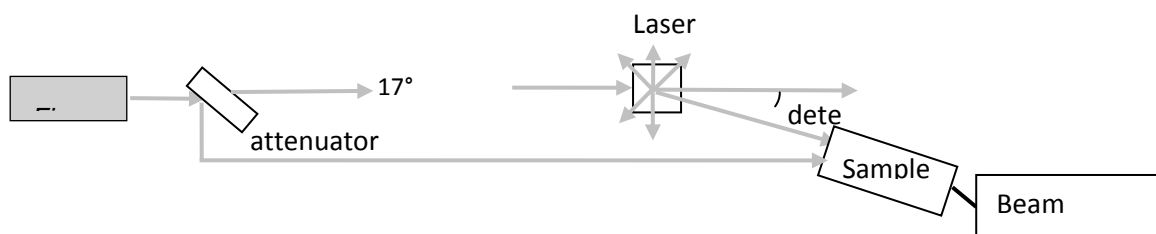
Figure A.2: Simplified scheme of optical configuration for zeta potential measurement on Zetasizer NanoZS

More details on the results produced in zeta potential measurements with M3-PALS technique are available in the documentation from Malvern Instruments. The reported value is the **average of zeta potential values from the 3 measurements** (determined during the fast field reversal step), with possible exclusion of diverging data. Degradation of the signal was observed on the phase plot during the measurement for some TiO$_2$ samples. In this case, only the first measurement was used.
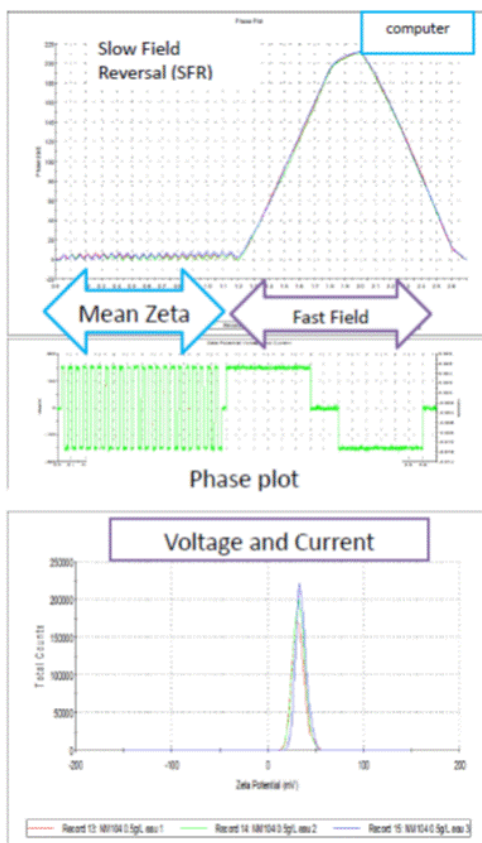
Figure A.3: Data plots retrieved from zeta potential measurements on Nanosizer ZS, example of 3 consecutive measurements on a suspension of NM104 at 0.5 g/L in pure water.

V. Comments on use and applicability

The current method describes the procedures applied at CEA. It can be transferred on other systems of apparatus or nanoparticles.

VI. References

A lot of support documents can be downloaded from http://www.malvern.com, application library section.

V

Appendix B : Standard Operating Procedure for "best dispersed state" suspensions of TiO2 and SAS

Camille Guiot and Olivier Spalla (CEA)

I.   *General description*

Prior to the determination of dispersion protocols, a study of zeta potential Vs. pH has been undertaken on NM suspensions in aqueous ionic media, in order to determine isoelectric points (IEP) and apprehend suspension stability depending on pH (cf ref 1, and internal report for NANOGENOTOX). In absence of steric stabilization, the pH range surrounding the IEP (pH of zeta potential reversion) is generally a zone of instability.

The results showed that the most stable TiO_2 suspensions are obtained for acidic pH (pH < 4), whereas Silica suspensions are more stable for pH above 5.

The objective of this protocol is to disperse NM in the conditions giving the **best dispersion state achievable** in order to access the size of smallest aggregates, *i.e.* **in acidic conditions for TiO_2 NP**, and **in pure water for Silica NP** (pH around 7, lowest ionic strength). We then assume that in any other dispersion conditions (with addition of serum, BSA, buffer *etc*.), any bigger aggregate would results from those specific conditions.

II.   *Chemicals and equipment*

- Weigh-scale (0.1 mg precision)
- Ultrasonicator, with 13 mm probe, placed in a sound abating enclosure, (Sonicator Sonics & Materials, VCX500-220V, 500 W, 20 kHz, standard 13 mm disruptor horn) or equivalent.
- pH-meter with conventional glass electrode (better if the electrode is dedicated to NP suspension measurements)
- standard 20 mL glass vial of internal diameter 24 mm (Figure B.1)
- volumetric glassware (10 mL jauged vial) and pipettes
- HNO_3 (analytical grade)
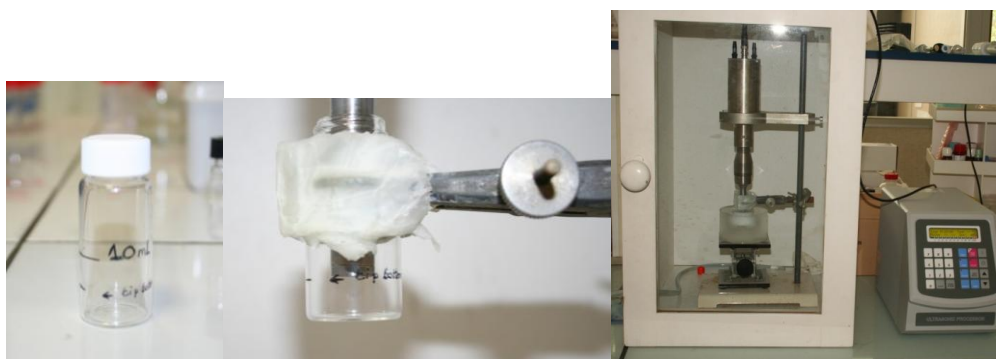- Purified water (MilliQ or Nanopure water)

Figure B.1: 20 mL vial and probe set up for ultrasonication of 10 mL suspensions.

III. Sample preparation

Brief

> For TiO$_2$ nanomaterials: Sonication of 3.41 mg/mL NM suspension in HNO$_3$ 10^{-2} mol/L acidic medium, 40% amplitude 20 min sonication in ice-water cooling bath.
>
> For Silica nanomaterials: Sonication of 6.82 mg/mL NM suspension in ultrapure water, 40% amplitude 20 min sonication in ice-water cooling bath.

TiO$_2$ nanomaterials

Detailed protocol:

- Preliminary prepare a solution of HNO$_3$ 10^{-2} mol/L in ultrapure water (Milli-Q)
- Wear lab coat, protective gloves, mask and glasses, and damp paper towel around the weigh-scale.
- Weigh 34.1 mg of TiO$_2$ NM in 20 mL standard glass vial,
- Add 10 mL of solution HNO$_3$ 10^{-2} mol/L
- Prepare the sonication set up with the vial and the sonicator fixed on some support in a way that the sonication probe is dipped in the suspension with its bottom at the middle of the suspension volume (height of liquid 11 mm). For easiness and better reproducibility, marks can be drawn on the vial and on a scale (figure B.1).
- Place a water/ice bath under the vial and adjust its level to best immerged the vial,
- Ultrasonicate for 20 min at 40% of power,
- Note down the time of the end of sonication (called t$_0$) and the energy released during the sonication process if available (press energy button on sonicators Sonics & Materials),
- The suspension is ready! For characterization of best dispersed state.

Synthetic Amorphous Silica

Detailed protocol:

- Wear lab coat, protective gloves, mask and glasses, and damp paper towel around the weigh-scale.
- Weigh 68.2 mg of silica NM in 20 mL standard glass vial,
- Add 10 mL of ultrapure water (Milli-Q)
- Prepare the sonication set up with the vial and the sonicator fixed on some support in a way that the sonication probe is dipped in the suspension with its bottom at the middle of the suspension volume (height of liquid 11 mm). For easiness and better reproducibility, marks can be drawn on the vial and on a scale (figure B.1).
- Place a water/ice bath under the vial and adjust its level to best immerged the vial,
- Ultrasonicate for 20 min at 40% of power,
- Note down the time of the end of sonication (called t0) and the energy released during the sonication process if available (press energy button on sonicators Sonics & Materials),
- The suspension is ready! For characterization of best dispersed state.

Energy of sonication

From the indication of energy given by the sonicator Sonics & Materials, it is possible to estimate the energy per mL, the power (total energy / time of sonication) and the power per mL delivered to the suspension. The energies were recorded systematically for each sample preparation, and the corresponding mean values and standard deviations are reported in the following table.

Table B.5: Mean values and standard deviations of energy, power, energy per mL and power per mL obtained from indications on the sonicator during the preparation of repeated samples.

20 min sonication of 10 mL suspension at 40% amplitude	Energy recorded from the sonicator (J)	Power (J/s or W)	Energy per mL (J/mL)	Power per mL (W/mL)
TiO_2 3.41 g/L in HNO_3 10^{-2} mol/L (36 samples)	35507.1 +/- 2168.5	29.59 +/- 1.8	3550.71 +/- 216.9	2.96 +/- 0.2
Silica 6.82 g/L in pure water (15 samples)	35670.3 +/- 618.6	29.73 +/- 0.5	3567.03 +/- 61.9	2.97 +/- 0.1

IV.   Comments on use and applicability

This protocol is used for characterization matters and is not suitable for dilution in biological media for toxicology studies for example. However it represents the first step of a three steps protocol implying pH-adjustment and subsequent addition of bovine serum albumin, developed within NANOGENOTOX as an alternative protocol to the validated NANOGENOTOX protocol.

The concentration of 3.41 g/L for TiO_2 was chosen to give 2.56 g/L with dilution of ¾ in a subsequent step of BSA addition.

The concentration used for Silica has been multiplied by 2 (6.82 g/L) for SAXS measurement concerns, where the contrast with Silica is lower than with TiO_2. It was also used to test a protocol with more concentrated suspensions for Silica. Nevertheless, a lower concentration shouldn't be a problem for other techniques, and could even lead to better dispersions.

After preparation of these "stock suspensions", further dilution (in HNO_3 10^{-2} M for TiO_2 and in ultrapure water for Silica) can be performed for specific sample preparation for a given characterization technique. For example a dilution by 100 is performed for preparation of samples for atomic force microscopy measurements.

The high sonication amplitude of 40% is needed to have the best dispersed state; however, it usually results in more contamination by black titanium residues from the probe. These residues are quite big and then settle very fast, so it might be better to wait 10 min before sub-sampling.

V. References

1. Guiot, C.; Spalla, O.; de Temmeman, P-J.; Mast, J.; Shivachev, B.; Birkedal, R.; Levin, M.; Nielsen, S.H.; Koponen, I.K.; Clausen, P.A.; Jensen, K.A.; Rousset, D.; Bau, S.; Bianci, B.; Witschger, O.; Motzkus, C.; *Nanomaterial datasets with requested physicochemical properties – Midterm Deliverable, Key intrinsic physicochemical characteristics of NANOGENOTOX nanomaterials.* KA Jensen and N Thieret (Eds.): August 2011; 44 pp.

Appendix C: Standard Operating Procedure for Dynamic Light Scattering (DLS) measurements and data treatment used for analysis of NANOGENOTOX particulate MN

Camille Guiot and Olivier Spalla (CEA), Keld Alstrup Jensen (NRCWE), Olivier Witschger (INRS)

I. General description

Dynamic Light Scattering (DLS), also called Photon Correlation Spectroscopy (PCS) or Quasi-Elastic Light Scattering (QELS), is a technique of characterization of colloidal systems based on the scattering of visible light resulting from the difference in refractive index between the dispersed colloids and the dispersion medium. The method may be applied for sizing particles suspended in a liquid in the range from about 0.6 nm to about 6 μm depending on the optical properties of material and medium.

The principle in DLS is measurement of fluctuations in laser light scattered by vibrating particles suspended in a liquid as function of time. The vibration is due to Brownian motion caused by collision with solvent molecules of the liquid. The Brownian motion varies as a function of particle size and causes variation in the intensity of scattered light as function of time. A correlator compares the signal measured at a time t_0 with different very short time delays dt (autocorrelation). As the particles move, the correlation between t_0 and subsequent dt signals decreases with time, from a perfect correlation (1) at t_0, to a complete decorrelation (0) at infinite time (order of milliseconds). In case of big particles, the signal changes slowly and the correlation persists for a long time, whereas small particles have high Brownian movement causing rapid decorrelation.

In fact a DLS instrument measures the velocity of Brownian motion, defined by the translational diffusion coefficient D of the particles. The particle size, or more precisely its hydrodynamic diameter d_h, is then estimated using the Stokes-Einstein equation assuming spherical shape:

$$d_h = \frac{kT}{3\pi\eta D}$$

k: Boltzmann's constant
D: translational diffusion coefficient
T: absolute temperature
η: viscosity

It should be noted that even if a particle is really spherical, the spherical DLS size is fundamentally different from the physical spherical size. The hydrodynamic size includes the double-layer with highly polarized water molecules around the physical particle. When the particle morphology is highly non-spherical, the hydrodynamic size should be understood as the equivalent hydrodynamic spherical size. Establishment of mean hydrodynamic size and size distributions (intensity, number, volume) is reached by DTS software algorithms, by fitting the correlation function (cf. data treatment section).

II. Chemicals and equipment

- Test material or chemical
- Dispersion medium
- Ultrasonic probe equipped with a standard 13 mm disruptor horn
  - at CEA: Sonics & Materials, VCX500-220V, 500 W, 20 kHz;
  - at NRCWE: Branson Bransonic 400W,
  - at INRS : Heilscher UP200H (200W with 14 mm Ti disruptor horn)
- Dynamic Light Scattering apparatus
  - at CEA, NRCWE: Zetasizer Nano ZS (Malvern Instruments), equipped with laser 633 nm, computer controlled by Malvern software (DTS 5.03 or higher), samples inserted in DLS cuvettes of clear disposable polymer (optical path length 1 cm) or glass cells or folded capillary zeta cells.
  - At INRS: VASCO™ particle size analyzer (VASCO-2 Cordouan Technologies, France) with a 65 mW fiber semiconductor laser at a wave length of 635 nm. Data collection and analysis is provided by the proprietary software nanoQ™ 1.2.0.4. The sample is directly dropped off (volume ≈ 2 µl) in the center of the cell with a pipette. The bottom of the cell is formed by the upper surface of the glass prism guiding the laser beam.
- Viscosimeter (e.g, Malvern Inc., SV-10 Vibro Viscometer) *Optional for measurement of true viscosities*
- Pipette and pipette tips
- Syringes and syringe filters or filter paper

Specificities for Zetasizer NanoZS from Malvern Instruments

DLS measurements rely on non-invasive back scatter (NIBS®) technology developed by Malvern Instruments, in which the signal is detected at 173° (Figure C.1). The signal is treated by a digital correlator, and transmitted to the computer. DTS software enables the fitting of correlation data either by a monomodal mode, called the cumulant analysis (as defined by ISO 13321 Part 8) to obtain a mean size (Z-average diameter) and a polydispersity index (PDI), or by a multiple exponential known as the CONTIN method to obtain a distribution of particle sizes.
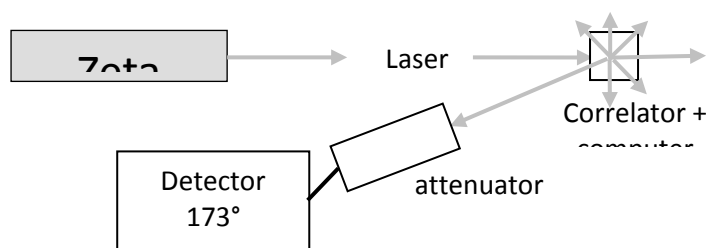

Figure C.1: Simplified sketch of the optical configuration for DLS measurement on Zetasizer Nano ZS

Specificities for Vasco Cordouan

The VASCO™ has an original design of the sample cell (thin layer technology) and optics arrangement. The configuration allows also the photo-detector to collect the back-scattered light signal at an angle of 135° (Figure C.2 below). In addition, the cell is hermetically closed by a mechanical system that includes a mobile glass rod with a photon trap. This rod can both absorb the excess of transmitted light and controls the sample thickness, down to few tens of microns. Lowering the thickness of the sample (and then volume of analysis) reduces significantly the probability for a photon to scattered several time. Thus, the multiple-scattering artifact is well reduced using this unique design. Also the thin layer technology prevents the sample from local heating.
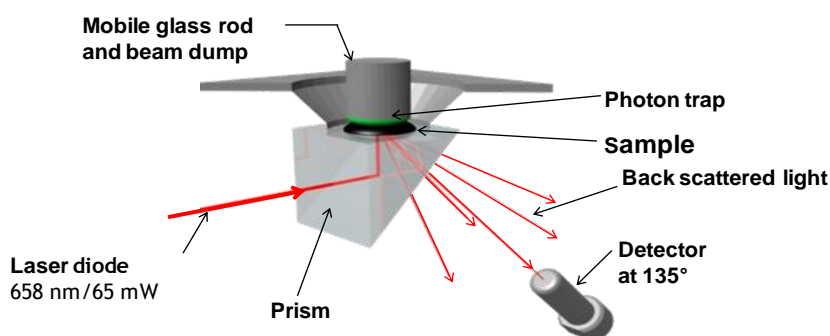
Figure C.2: Configuration for DLS measurement on VASCO™

The NanoQ™ software proposes two acquisition modes:

- Continuous mode where the data acquisition is stopped by the user.
- Statistical mode where successive data acquisitions are performed automatically following a pattern set by the user (ex. 15 successive acquisitions of 60s each).

The NanoQ™ software enables to use two different algorithms for data analysis:

- Cumulants method (according to ISO 13321) for mono-disperse samples. The monomodal analysis of the autocorrelation function provides only a mean size value (light scattering intensity-averaged diameter also named as Z-averaged diameter) and a measure of the broadness of the distribution through the polydispersity index (PdI).
- Padé-Laplace method for polydisperse samples. This method makes no hypothesis as to the number of components for multi-exponential analysis. This method gives as a result a discrete density of intensities (histogram), each of them corresponding to a given hydrodynamic diameter. Volume and number histograms are also available based on the Pade-Laplace analysis combined with a Mie algorithm. The NanoQ™ does not provide results express as continuous distribution curves for polydisperse samples.

Co-funded by
the Health Programme
of the European Union

III. Sample preparation

Dispersions for analysis are prepared by mixing particulate material into a liquid dispersion medium. A sub-sample of a suitable concentration is added to suitable measurement cuvettes. Dispersions are typically produced by sonication in a dispersion medium (see each dedicated SOP for specific dispersion protocols). The dispersion medium must be filtrated before use to avoid any dust contamination. This can be done by using syringe filters or filter paper with high efficiency. Usually filters with a 0.2 to 0.45 μm pore-size are sufficient for filtration of dispersion media.

The concentration required for analysis depends in part on the relative refractive index between particles and dispersion medium, the particle size and polydispersity and the sample absorption. Malvern apparatus is designed to measure samples over a large range of concentration and size of particles. Specifications of sample properties (concentration range, size of nanoparticles, medium) can be found in the documentation from Malvern Instrument accessible on their website. It is mandatory that the dispersion is stable within the time-frame of the measurement.

IV. Measurements

Brief

> **Measurements are performed at ambient temperature according to the procedure appropriate for each type of apparatus. Sample properties such as material and dispersant refractive indices and viscosity are entered in the software for analysis. Number and duration of run and optical configuration are automatically optimized by the software for Malvern apparatus. For Cordouan apparatus, 15 runs of 60s are performed.**

On ZetaSizer NanoZS from Malvern Instrument

DLS measurements can be performed in disposable polystyrene cuvettes (optical path 1 cm, volume 1 mL) or alternatively glass cuvettes (at NRCWE) or in semi micro polystyrene disposable cuvettes (optical path 1 cm, volume 500 μL) or in clear disposable zeta cells DTS1061 just before zeta potential measurements (at CEA). The measurements are repeated 3 (CEA) or 6 (NRCWE) times with automatic determination of duration and number of runs, and averaged. The repeated analyses are conducted to enable omission of measurements with bad correlation data or abnormal solutions to the correlation function (must be carefully considered).

The following procedure is recommended as the general approach for DLS measurement of NM dispersions.

- Turn on the computer and DLS instrument
- Allow the instrument to warm up according to the manufactor's recommendation (30 min)
- *Optional: Complete viscosity measurement using the SV-10 Vibro Viscometer mounted with the 10 ml flow-reactor placed in a thermostated water jacket. The measured dynamic viscosity is used as input data for the specific dispersion measured in the DTS software.*
- Upload the DTS software and the "Measurement" window for entering material specific data on dispersion medium and test material as well as specific analytical settings :
  - Refractive index and absorption values for dispersant and NM (cf Tables C.1 and C.2)
  - Temperature conditions (25°C) and equilibration time for measurement

XIII

- o The General purpose model is selected for initial evaluation of data and is the most generic model for calculation of size.
- Select a sample cuvette and ensure that it does not contain dust, nor defects or scratches in the measurement area of the cuvette. Some producers have been found to deliver cuvettes with scratches or folding structure in the measurement area at one side of the cuvette. Dust may be cleaned out by rinsing the cuvette in dispersion medium.
- Fill in a suitable volume of the dispersion into a suitable measurement cuvette using a pipette
- Place the sample cuvette in the sample holder in the DLS instrument
- Run analysis (click "play" on the measurement window)
- The size analysis may be immediately accepted if the DTS Expert advice denotes the result quality as "Good". If the result is not of good quality, the sample should be further analyzed for presence of dust, cuvette errors, large particles, sedimentation, wall-deposition etc.
- If the sample contains particles with large spread in size distribution, one may consider filtering the sample through different syringe filters to investigate presence of small nm-size particles. Small nm-size particles may not be fully resolved when coarser particles are present due to the large drop (10^6 per decade) in scattered light intensity with size.
- If parameters such as refractive indexes, absorption coefficient or viscosity were wrong or unknown at the measurement time, the correction can be made afterwards using the command Edit (right click on the measurement) in DTS software.

The measurement conditions generally used at CEA and NRCWE are listed in Table C.1 and C.2.

The viscosity considered for measurement is generally the one of pure water but the data can be corrected afterwards for the values measured.

At CEA, the viscosity of the dispersions could not be measured. Therefore, the viscosity of water was used for all dispersions prepared without addition of BSA or in the pH-adjusted protocol (Table C.1). For suspensions prepared according to the generic NANOGENOTOX protocol, all data were corrected considering the real viscosities measured by NRCWE (usually around 0.99 cP – 1 cP).

Table C.1 Conditions used at CEA, refractive index (R_i), absorption or imaginary part (R_{abs}) and dynamic viscosity for MN in optimized dispersions.

	Water (STP)	TiO$_2$	Silica$_{(amorphous)}$
R$_i$	1.33	2.49	1.50
R$_{abs}$		0.01	0.01
Viscosity [cP]	0.8872	water	water

Table C.2 Conditions used at NRCWE, refractive index (R_i), absorption or imaginary part (R_{abs}) and dynamic viscosity for MN in optimized dispersions.

	Water (STP)	Rutile	Anatase	Silica$_{(amorphous)}$	CNT
R$_i$	1.33	2.903	2.49	1.544	2.02
R$_{abs}$		0.10	0.10	0.20	2.00
Viscosity [cP]	0.8872	water	water	water	variable

XIV

DLS measurements for stability over time

DLS measurements for stability over time are performed on 500 µL suspension in semi micro polystyrene cuvette (CEA) or 1 mL in standard disposable cuvette (NRCWE). The first measurement at t_0 is performed as usual DLS measurements (described above) with automatic determination of parameters. The number of run, duration, position and choice of attenuator are then recorded and used for the following measurements, which are scheduled over a period of approximatively 16 h, usually every 30 min.
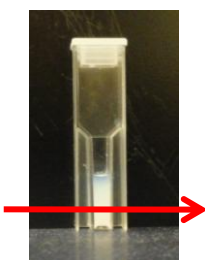
Figure C.3: semi micro cuvette used at CEA for DLS measurements over time. The arrow represents the position of the laser beam probing the suspension.

On Vasco™ from Cordouan Technologies

The following procedure was used and is recommended:

- Turn on the Vasco™ and wait about 30 minutes before starting a measurement.
- Run the NanoQ™ software, enter the material specific data on dispersion medium and test nanomaterial as well as specific analytical settings (see table below). Temperature is set to 21 °C.
- Prior to start any measurement, it is strongly recommended to clean the cell carefully in order to prevent pollution from previous measurement. The cleaning operation has to be made gently according to the manufacturer recommandations.
- Once the cell is perfectly clean, introduce the sample to analyze. For that, use a plastic pipette to extract a sample from the suspension to analyze and drop off a small volume (≈ 2 µl) in the center of the cell as shown on the picture below. In order the perform measurements in good conditions, the suspension to be analyzed should cover entirely the bottom of the cell, as this correspond to the upper surface of the glass prism guiding the laser beam. For the suspensions analyzed in the NANOGENOTOX Joint Action, the thickness of the liquid was set to about 1.5mm (position "up" of the dual thickness controller). After closing the mechanical system, the measure procedure itself can begin.

  - Run the analysis.
  - Process the data.

The conditions used at INRS for the analysis with the Vasco™ are reported in the following table.
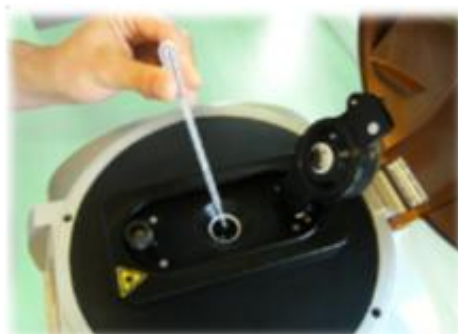
Figure C.4: Illustration of sample deposition on Vasco^{TM} apparatus.

Table C.3 Conditions used at INRS, refractive index (R_i), absorption or imaginary part (R_{abs}) and dynamic viscosity for MN in optimized dispersions.

	Water	TiO$_2$	Silica$_{(amorphous)}$
R$_i$	1.33	2.49	1.54
R$_{abs}$		0.1	0.2
Viscosity [cP]	0.97	0.97	0.97

For all measurements performed with the Vasco™ within the NANOGENOTOX Joint Action, the "statistical mode" was used, i.e. 15 successive measurements with a time duration of 60 s each.

V.   Data treatment

Brief

A monomodal model, called the cumulant analysis is used to treat the raw data correlograms (decaying as exponential). It determines a Z-average (diameter of particles scattering with higher intensity) and a polydispersity. Since these samples are quite polydisperse, more sophisticated models, such as the CONTIN method, are applied as multimodal analysis to reveal size distributions.

On ZetaSizer NanoZS from Malvern Instrument

The actual raw data obtained from a dynamic light scattering experiment is the autocorrelation function, which is an exponential decaying with a characteristic time related to the size of the diffusing object. An example of correlation data is shown on Figure C.5 for two NM104 samples (0.5 g/L TiO$_2$, 0.036 mol/L of monovalent salt), one stable suspension at pH 2.8 (red curves) and the supernatant of an aggregated sample at pH 10.1 (green curves). The data used are the averaged data for 3 consecutive measurements.

XVI

Co-funded by
the Health Programme
of the European Union

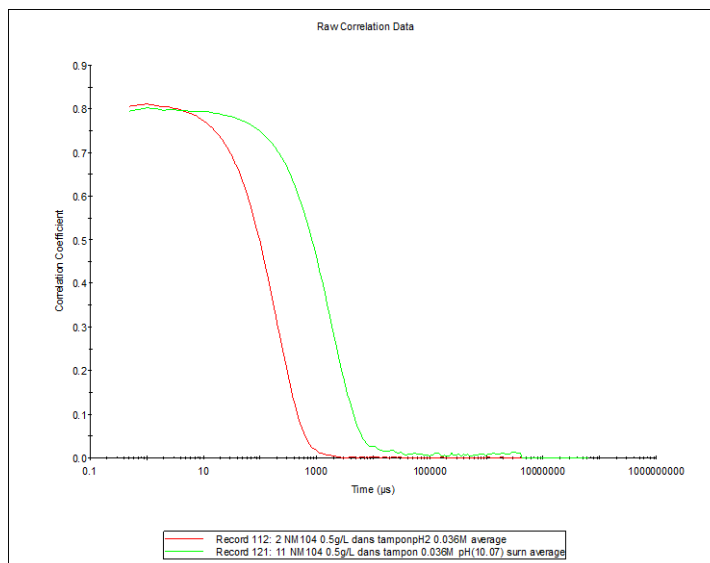*Figure C.5 : Example of raw correlation data for two NM104 samples (0.5 g/L TiO$_2$ in 0.036 mol/L ionic buffer), one stable suspension of relatively dispersed particles at pH2.8 (red curve), and one unstable sample of big aggregates at pH10.1 (green curve, measure on supernatant).*

The raw correlation data are analyzed to extract information on size and distribution. Various algorithms can be used.

The simplest one is called the *Cumulants analysis*. It fits the data by approximating the single exponential decay by a degree 2 Taylor development function. This provides a **Z-average** mean value, which corresponds to the particle size diffusing with the highest intensity, and a **polydispersity index (PDI)** for this monomodal distribution. In DTS software, the corresponding graph is entitled "Cumulants fit". This analysis method applies for monomodal distributions with polydispersity lower than 0.25, and is in agreement with ISO 13321 standard. In case of higher polydispersity, these two parameters, Z-average and PDI, are not sufficient to describe precisely the size distribution of the sample and a multimodal analysis is necessary.

Some examples of Cumulant fits analysis applied to NM104 samples are displayed in Figure C.6. The high PDI obtained for the sample at pH 10 indicates that this model is not advanced enough to determine an accurate size distribution for this sample.

For polydispersity indices between 0.08 and 0.5, the correlation data can be better analyzed by the *CONTIN method*. It consists in fitting the correlation data by the best combination of a set of 24 exponential functions, giving rise to a size distribution over 24 granulometric classes. In DTS software, this fit is denominated as "distribution fit", "data fit" or "size fit" (Figure C.7).
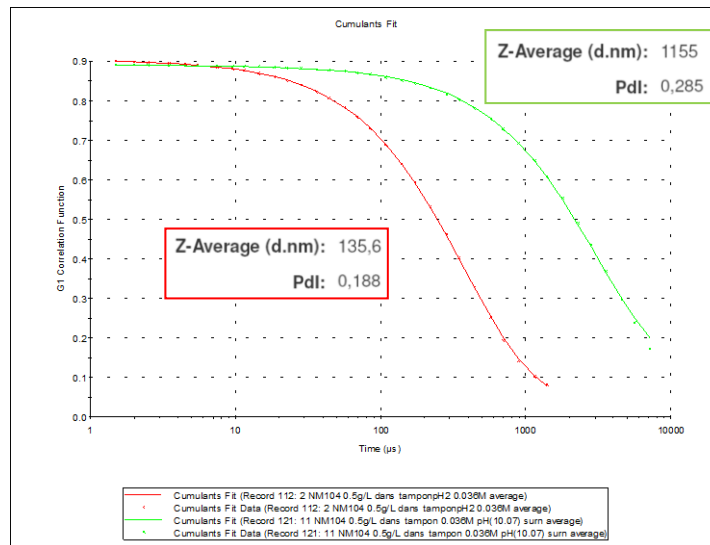
Figure C.6: Data and fits by the Cumulant method, together with calculated values of Z average and polydispersity, for two NM104 samples (0.5 g/L TiO$_2$ in 0.036 mol/L ionic buffer, stable suspension at pH2.8 in red and unstable sample of big aggregates at pH10.1 in green).
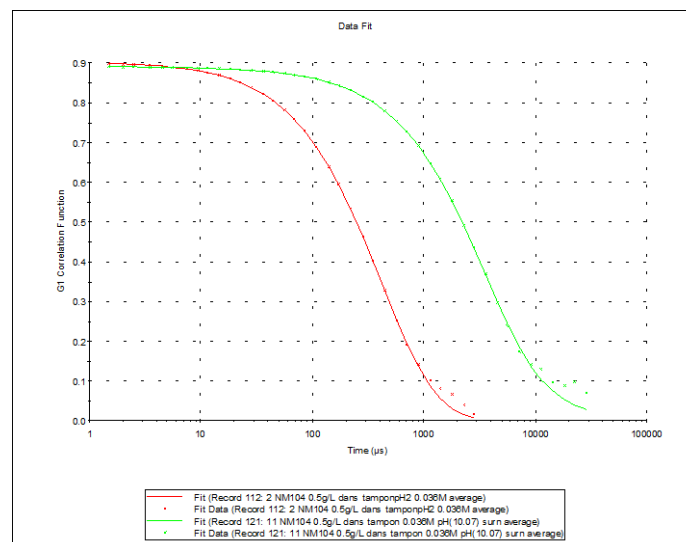
Figure C.7: Data and fits by the CONTIN method, for two NM104 samples (0.5 g/L TiO$_2$ in 0.036 mol/L ionic buffer, stable suspension at pH2.8 in red and unstable sample of big aggregates at pH10.1 in green).

Taking into account the refractive indices of material and dispersant, Mie Theory can be applied to represent size distribution in **volume**. The **number** size distribution can then be calculated from simple geometrical considerations (Figure C.8). Distribution data can be retrieved from DTS software in the form of tables of diameter, percentage and width for the three main peaks.

XVIII
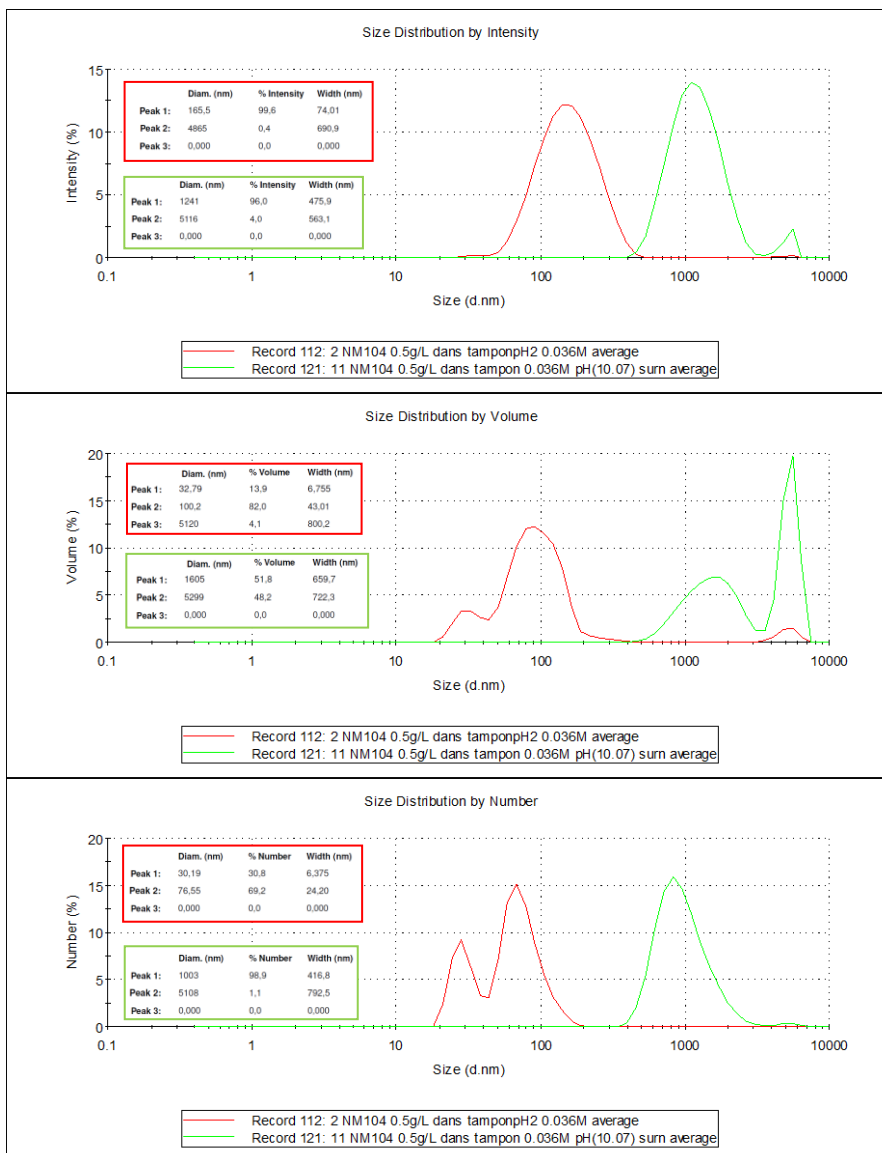
Figure C.8: Size distributions by intensity, by volume and by number, together with tables of numerical values for the three main peaks of each distribution, for two NM104 samples (0.5 g/L TiO2 in 0.036 mol/L ionic buffer, stable suspension at pH2.8 in red and unstable sample of big aggregates at pH10.1 in green).

It has to be noticed that for 2 particles with a size ratio of 10, the contribution of the bigger particle to the volume distribution is 10^3 times more than the smaller one, and it reaches 10^6 for the distribution by intensity. Since the measurement done by DLS is based on the intensity, this means that the light scattered by a few large particles may totally cover the signal from the smaller ones.

After controlling correlation data and fits, an average measurement is calculated with the software. As an example, the main graphs observed for the 3 initial measurements of a sample of NM104 at pH

XIX

2.8 (0.5 g/L TiO$_2$, 0.036 mol/L of monovalent salt) are displayed on Figure C.9. Since the correlation data are good, all 3 measurements are taken into consideration for the averaged data.
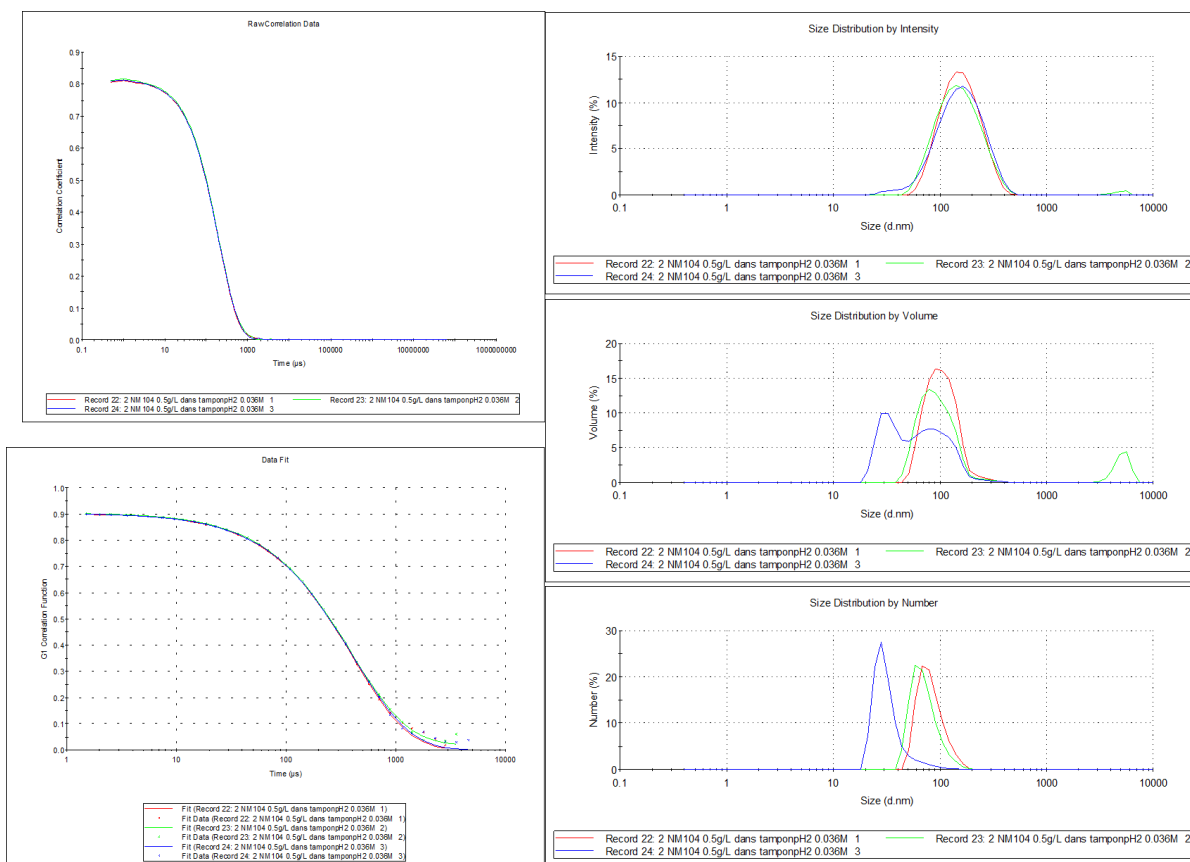
Figure C.9: Main graphs reported by DTS software for 3 consecutive measurements of a NM104 sample (pH 2.8, 0.5 g/L TiO$_2$ in 0.036 mol/L aqueous ionic medium)

The main parameter reported in the results section is *"Z-average"*, which represents the mean size contributing to the major part of the signal **in intensity**. For polydisperse samples, this value mostly gives a hint on the aggregation state of the particles but does not reflect the hydrodynamic size of most of the dispersed particles (in number), which of course is much lower. When Z-average is higher than approximately 500 nm, it can only be deduced that there are big aggregates in suspension but the numerical value is usually meaningless.

VI. Comments on use and applicability

DLS is very suitable for size and stability analysis of particles in liquid dispersions. However, great care should be taken in interpretation of data; especially when the sample contains both µm- and small nm-size particles.

XX

For better accuracy of size-determination, it is important to obtain true values of the optical properties and viscosity of the dispersion liquid.

Currently, there is high uncertainty in understanding the signal obtained during analysis of dispersions of CNT. Due to this uncertainty, it was decided that a generic SOP for DLS analysis of CNT by DLS could not be made as part of the NANOGENOTOX project.

VII. References

A lot of support documents can be downloaded from http://www.malvern.com, application library section.

XXI

Appendix D: Standard Operating Procedure for Small Angle X-ray Scattering measurements on NM suspensions and data treatment by fitting with a model for aggregates

Camille Guiot and Olivier Spalla (CEA),

This appendix describes the general procedure applied at CEA LIONS to perform Small Angle X-ray Scattering measurements and to treat the data to extract physic-chemical properties of materials. This procedure was applied in the framework of NANOGENOTOX to characterize TiO_2, Silica and CNT manufactured nanomaterials as raw powders and TiO_2 and Silica in aqueous suspensions.

I.   General description

Here is a brief presentation of SAXS technique, for more details on this technique, cf references at the end of this document.

Small-Angle X-ray Scattering is a technique based on the interaction between X-rays and electrons to probe the structure of materials. The processed data is the number of X-ray scattered by a sample as a function of angular position of a detector (Figure D 1).
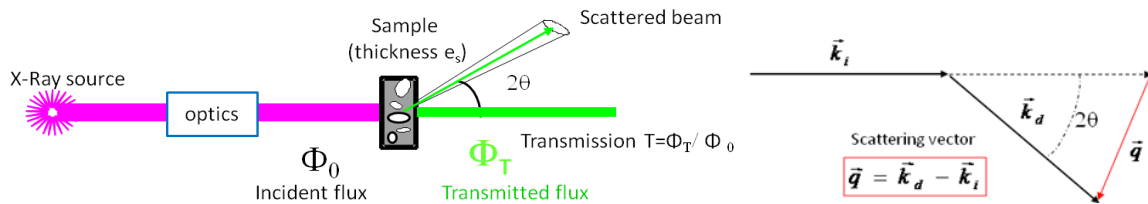
Figure D 1: Schematic set up for SAXS and physical quantities

2D raw data images are converted into diffractograms displaying the **scattered intensity I as a function of scattering vector q** defined by:

$$q = \frac{4\pi \, sin\theta}{\lambda}$$

λ : X-ray wavelength

The experimental scattering intensity is defined as the differential scattering cross-section per unit volume of sample and can be expressed as follows:

$$I(q) = \frac{1}{V}\frac{d\sigma}{d\Omega} = \frac{\eta_1 C_{ij}}{\eta_2 (\Phi_0 ST)dt}\frac{1}{\Delta\Omega}\frac{1}{e}$$

σ : scattering cross-section

V : volume of sample

C_{ij}: number of counts detected on a pixel ij during dt

η_1: detector quantum efficiency when measuring the direct beam

η_2: detector quantum efficiency for the count Cij

$(\phi_0 ST)$: flux (in detector unit counts/s) integrated over the whole beam transmitted by the sample

T: transmission of the sample

$\Delta\Omega$: solid angle covered by one pixel seen from the center of the sample ($\Delta\Omega = p^2/D^2$ with p the pixel size and D the sample to detector distance)

The intensity is then expressed in **absolute scale** (in cm^{-1}) to be independent of the experimental set up parameters (X-ray wavelength, experimental background, time of acquisition, sample thickness, etc).

General theorems of experimental physics have been developed to extract different properties of nanostructured material from the diffractograms, such as, shape of nanoparticles, surface area, interactions occurring, etc. *I(q)* curves can also be theoretically calculated from assumed nanostructures to fit the experimental curves.

In the simple case of binary samples, the scattering intensity is proportional to:

- the electronic contrast, more precisely the square of scattering length density difference between the two materials *$(\Delta\rho)^2$*,
- the concentration of the scattering object (in volume fraction), in case of suspensions for example.

Ultra Small Angle X-ray Scattering (USAXS) measurements give access to X-ray scattering data for a range of smaller *q* and then complement the SAXS diffractograms. It requires a specific and very precise set-up, different from the one used for SAXS.

Equipment

The experimental set up (X-ray source, optical elements, detectors, etc) and the procedure for absolute scaling of data has been thoroughly described by Zemb (1)and by Né (2).

Apparatus

The main set up components used for SAXS and USAXS experiments at CEA/LIONS are listed hereunder:

- X-ray generator : Rigaku generator RUH3000 with copper rotating anode (λ= 1.54 Å), 3kW
- Home made optic pathways and sample holders (with two channel-cut Ge (111) crystals in Bonse/Hart geometry for USAXS set up, cf Lambard (1992).
- Flux measurement for SAXS set up : pico amperemeter Keithley 615
- Flux measurement for USAXS set up : DonPhysik ionization chamber
- Detector for SAXS set up : 2D image plate detector MAR300
- Detector for USAXS set up: 1D high count rate CyberStar X200 associated to a scintillator/ photomultiplier detector.

All experiment parameters are monitored by computer thanks to a centralized control-command system based on TANGO, and interfaced by Python programming. 2D images are treated using the software *ImageJ* supplemented with some specific plugging developed at CEA/LIONS. This control-command system has is described in reference 5.

Calibration

A sample of 3 mm of Lupolen® (semi crystalline polymer) is used for the calibration of the intensity in absolute scale, the maximum intensity being adjusted to 6 cm^{-1}.

A sample of 1 mm of octadecanol is used for the calibration of the q range (calculation of sample-to-detector distance), the position of the first peak standing at 0.1525 Å^{-1}.

Calibrations in intensity and in q range are performed before each series of measurements.

II.   Sample preparation

Almost any kind of material can be analyzed by SAXS, whether it comes as a powder, a colloidal suspension, a gel, or even self-supported hybrid materials, and as long as the sample prepared meets some requirements of transmission and scattering properties.

Indeed, depending on the X-ray absorption coefficient of the material and its scattering properties, the sample thickness have to be adjusted to get a transmission as close as possible to the target transmission of 0.3 (optimal absorption/transmission ratio).

The sample thickness *e* is directly linked to the transmission *T* by the following equation:

$$e = -\frac{1}{\mu}\ln{(T)}$$

µ: X-ray absorption coefficient of the material,
T: transmission, *T* = transmitted flux/ incident flux of the direct beam

If not self-supported (liquids, powders or gel), the material to be analyzed is inserted in a cell, which can be made of glass (capillary), or X-ray transparent material such as Kapton® (polyimide). In any case, a measurement of the empty cell is performed and subtracted as a background for the sample measurement. See *Figure D 2* for examples of cells used at CEA/LIONS.

Powders

The coefficient of absorption depends on the material and on the energy. For the Cu Kα emission (8 keV) that is used on our setup, the coefficient for TiO$_2$ is μ_{TiO2} = 470 cm^{-1} , it is μ_{SiO2} = 77 cm^{-1} for Silica and μ_{CNT} is estimated to 6 cm^{-1}. The optimal sample thickness (equivalent thickness of dense material) to get a transmission of 0.3 is 25 µm for TiO$_2$, 150 µm for Silica and 2 mm for CNT.

In a first place, the TiO$_2$ powder samples were prepared between two sticky kapton® films pressed on a 0.4 mm brass cell (typical thickness of dense material around 30 µm). However, it was inferred that the presence of glue may affect the calculation of specific surface area of powders. Therefore, in a subsequent step, all the TiO$_2$ powder samples were measured in a flattened polyimide capillary,

mounted on a circular sample holder (**Erreur ! Source du renvoi introuvable.**, 2). The typical equivalent thickness of dense material obtained is 30 µm.

Most of the silica powder samples were prepared in 1.5 mm glass capillaries leading to typical equivalent thickness of dense material from 100 to 200 µm. However, NM203 powder is very sticky and was very difficult to insert into capillaries, so it was measured in a double sticky kapton® cell.

CNT powder samples were prepared in 5 mm thick or 15 mm thick cells sealed with two sticky kapton films. NM400 and NRCWE006 are very fluffy materials and therefore require the thicker cells.
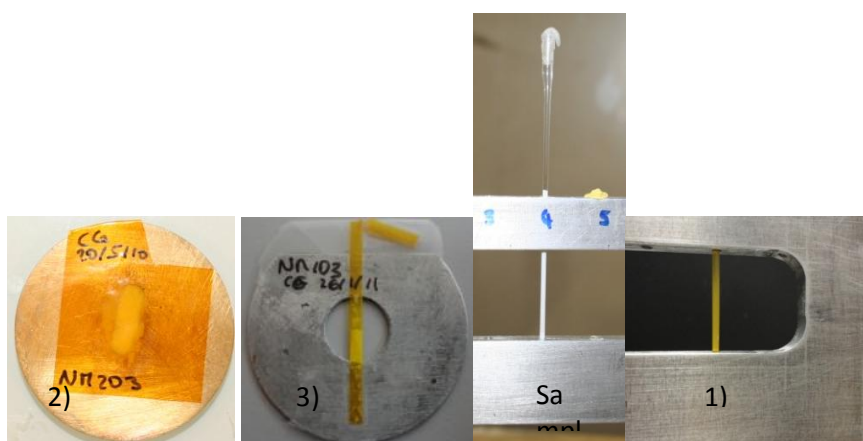
Figure D 2: Examples of different type of cells used for SAXS measurements, 1) double sticky kapton® cell for powders, 2) 1.5 mm flattened polyimide capillary for powders, 3) 1.5 mm glass capillary for powder or liquid samples, 4) 1.5 mm polyimide capillary for powder or liquid samples

Aqueous suspensions

The usual thickness of aqueous samples for SAXS measurement is 1mm with an acquisition time of 1 hour.

Dispersions for analysis are typically produced by sonication in a dispersion medium. The concentration required for analysis depends on the relative scattering length densities between particles and dispersion medium, and the density of materials. The sample must be stable within the time-frame of the measurement.

Typical concentration in oxide for NANOGENOTOX suspensions is 3 g/L. Since the scattering length density of silica is much lower than titania, higher concentrations were used when possible.

III. Measurements

In order to calculate the sample transmission, the flux of incident and transmitted beam are measured and averaged over 200 s before running the SAXS measurement.

The time of acquisition necessary for SAXS experiment depends on the sample properties. For Silica and TiO_2 powders, two measurements were performed: one with a short time of 200 s or 150 s to get unsaturated data for small angles (low q), and one for a long time of 1800 s to get data in the high q region with low signal/noise ratio. For CNT, the short time used was usually 60 s, and the long time 1800 s.

For aqueous suspensions prepared for NANOGENOTOX, SAXS measurements were performed in kapton capillaries of internal thickness 1.425 mm and run for 3600s, leading to transmissions of about 0.25. USAXS measurements were performed in 1 mm or 1.5 mm non-sticky double kapton cells (*Figure D 2*).

IV.   Data treatment

Brief

Raw data, translated into intensity as a function of the scattering vector q, are first normalized by parameters of the experiments such as acquisition time, sample thickness and calibration constants determined using reference samples. The data are thus expressed in absolute scale (cm^{-1}). Backgrounds are then subtracted. SAXS data obtained for short time and long time are concatenated, together with USAXS data to get continuous diffractograms on the whole q range.

On powder samples, the Porod law is applied to extract specific surface areas of raw materials. Data from suspensions are fitted with a model describing fractal aggregates of primary particles. In this model, the whole q range is divided into sections reflecting different structural levels in the sample, and fitted by local Porod and Guinier scattering regimes. Intensity average parameters are then determined such as radius of gyration for the primaries and for the aggregates, and a fractal dimension for the aggregates. Invariants are calculated, which give a correlation between the sample concentration and the specific surface area obtained in suspension.

Raw data treatment

SAXS data

Radial averaging of 2D image (ImageJ)

2D images from the detector are converted into Intensity = f(scattering vector q) graphs thanks to the software ImageJ together with SAXS plugging. The process follows mainly these steps:

- Determination of the center coordinates (direct beam position)
- Application of a mask to remove pixels corresponding to the beam stop and around the photodiode
- Radial averaging of the intensity, knowing pixel size, sample-detector distance and wavelength (example of parameters in Figure D 3), conversion of pixel position into scattering vector *q*, and creation of a .rgr file containing with *I(q)* data.
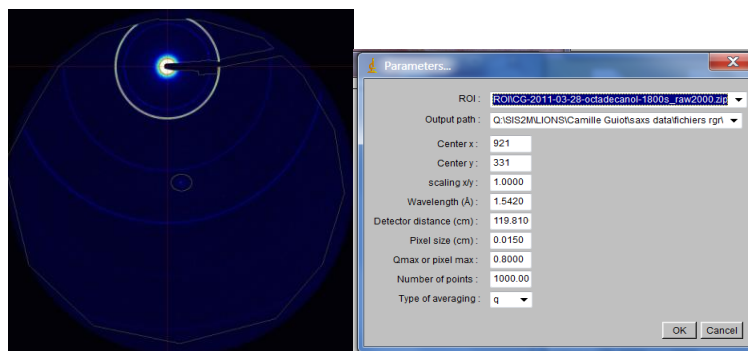
Figure D 3: Example of raw 2D image (octadecanol) and parameters used for radial averaging with ImageJ

Absolute scaling of I(q) (pySAXS)

In order to scale the data to the absolute scale in cm^{-1}, *I(q)* data generated by *ImageJ* as .rgr files are treated thanks to a homemade program called *pySAXS* and based on python programming.

The scaling involves a subtraction of the detector background and normalization by exposition time, sample transmission, sample thickness and K constant. The K constant is calibrated with Lupolen® sample and allows conversion of intensity in photon/s into absolute intensity in cm^{-1}. Example of parameters used for the scaling is shown on Figure D 4.

The subtraction of the empty cell signal and the normalization by the sample thickness can be done in a subsequent step.

USAXS data

Raw USAXS data are generated as intensity vs angle data in .txt files. Data treatment is achieved using *PySAXS* and involves the following steps:

- Subtraction of the "rocking curve" (signal with empty cell) normalized by the intensities at 0° (transmission).
- Desmearing, taking into account the effective size of the "punctual" detector (cf reference 3)
- Conversion of angle into q range
- Normalization by the sample thickness.

Co-funded by
the Health Programme
of the European Union

Figure D 4: Example of SAXS scaling parameter file from PySAXS software

Data analysis

General theorems of X-ray scattering have been developed to analyze SAXS data. Here are presented some simple laws for **binary systems** (two phase samples), that may be of use in NANOGENOTOX framework.

Porod's Law

In the high q range, sample diffractograms display an intensity decreases in a q^{-4} trend, called the "Porod region". This region corresponds in the "real space" to the scale of the interfaces (for smooth interfaces).

Therefore, for a binary sample, the asymptotic limit of the so-called "Porod's plateau", when data are represented in Iq^4, is related to the total quantity of interface Σ (in m^2/m^3) between the two phases, as follows:

$$\Sigma[m^{-1}] = \frac{\lim_{\text{plateau}}(I.q^4)}{2\pi(\Delta\rho)^2}$$

Where $\Delta\rho$ is the difference in scattering length density between the two phases. For a binary sample of **known thickness**, the volume fraction of a material φ_A, its specific surface area S_A/V_A (surface developed/ volume of A in the binary sample) and Σ are linked by the following relation:

$$\Sigma[m^{-1}] = \frac{S_A}{V_A}\varphi_A$$

For example, for a suspension of oxide in water, the determination of Porod plateau gives access to the concentration of the sample if the specific surface area of particles suspended is known (and vice versa).

XXVIII

Co-funded by
the Health Programme
of the European Union

Specific surface area determination from SAXS on powders

To treat raw SAXS data and get absolute intensities, one needs to normalize the intensity by the thickness of the scattering material. However, in powder samples, the sample thickness is not clearly defined and cannot be precisely controlled since it depends on the powder compaction and the different scales of porosity. To elude this problem, a model system is used, in which we consider the effective thickness of material crossed by X-rays, called e_B, corresponding to an equivalent thickness if all the material was arranged in a fully dense (no inner or outer porosity) and uniform layer .

The sample transmission is related to this equivalent thickness by the following equation:

$$e_B = -\frac{1}{\mu}\ln\left(T_{exp}\right)$$

Where μ is the material absorption coefficient for X-Ray (μ_{TiO2} = 470 cm^{-1} - μ_{SiO2} = 77 cm^{-1} [1] - μ_{CNT} = 6 cm^{-1}) and T_{exp} is the **experimental transmission** (transmitted flux Φ_T/ incident flux Φ_0), i.e. transmission of the sample with regard to the transmission of the empty cell (kapton® alone, empty capillary, etc). The intensity scaled by this thickness e_B is called I_1. The Porod's law can then be applied for I_1 to access the specific surface area of the powder. Cf reference 3 for more details on the data analysis.
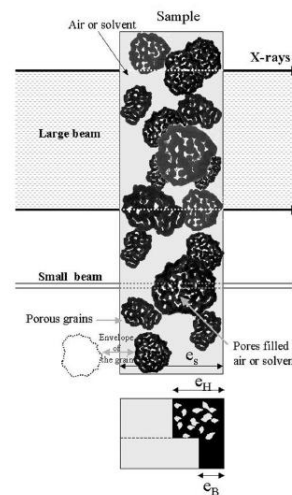
Figure D 5: Schematic representation of a powder sample for SAXS measurement, and definitions of equivalent thicknesses e_H and e_B.

Invariant theorem

When *I(q)* can be extrapolated to zero values of *q* (no interaction at a large scale, *i.e.* a flat signal for low q) and at infinite *q* (usually with the Porod law), the following invariant theorem can be applied:

$$Q = \int_0^\infty I_{Abs}\, q^2 dq = 2\pi^2\varphi(1-\varphi)(\Delta\rho)^2$$

This implies that the invariant *Q* is a constant for a defined composition, which gives access to the volume fraction φ, or to the evolution of interactions for a fixed composition.

Guinier regime

For **dilute samples of monodisperse objects** (negligible position correlation between scattering objects, i.e. structure factor 1), the intensity in the low q region (qR_G<<1) can be approximated to:

$$I(q) \approx A\left(1 - \frac{(qR_G)^2}{3} + Bq^3\right)$$

Which gives access to the **radius of gyration of the particles R_G** with the slope of ln(*I*)=f(q²).

Co-funded by the Health Programme of the European Union

Data fits

Assuming values of parameters such as volume fraction, size, shape and polydispersity of scattering objects for a model sample, it is possible to calculate theoretical curves of *I(q)*. Therefore, the adjustment of such parameters to fit experimental curves allows for the modelisation of the sample properties.

Unified model of aggregates in suspension for SAXS data treatment

A unified fitting approach, developed by Beaucage et Al. (5,6,7,8) was used to treat X-ray scattering data from TiO_2 and Silica suspensions composed of agregates of primary particles.

In this model, the whole q range is divided into sections reflecting different structural levels in the sample, and fitted by local Guinier, fractal and Porod scattering regimes. An example is illustrated on Figure D 6.

It is reminded that the scattering vector *q* is homogeneous to the reverse of a length, so large q values actually corresponds to small observation scale in the direct space.

For a smooth surface of primary particles, **at large q** (the scale of interfaces) the intensity decays as a power-law of q^{-4} defining the Porod regime:

$$I_{Porod\,1}(q) = B_1\,q^{-4}$$

The prefactor B_1 is directly linked to the specific surface area of the primary particles:

$$B_1 = 2\pi N(\Delta\rho)^2 S$$

With *N* and *S* respectively the number density and the average surface area of primary particles and $\Delta\rho$ the difference of scattering length density between scattering object (TiO_2 or Silica) and medium (water).

This Porod regime is preceded **at lower q** by a Guinier regime, signature of the size of primary particles, and is described by:

$$I_{Guinier\,1}(q) = G_1 \exp\left(\frac{-q^2 Rg_1{}^2}{3}\right)$$

XXX
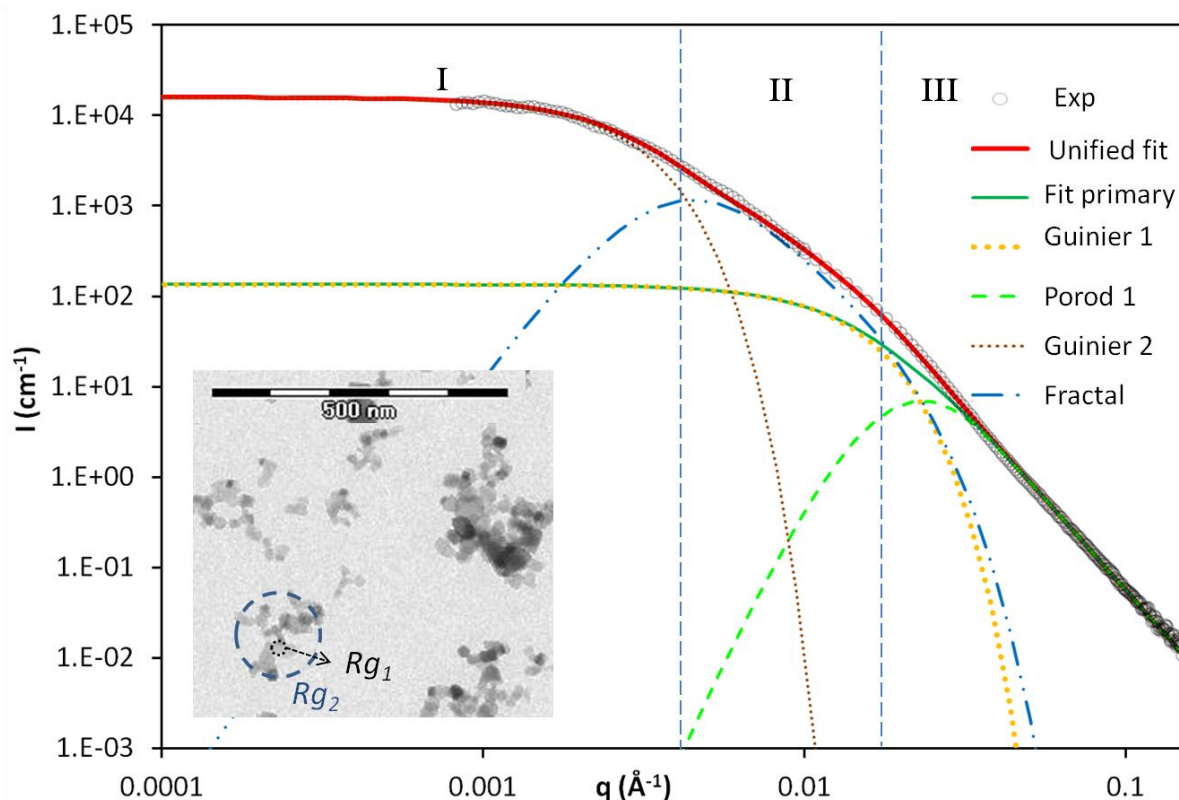
Figure D 6: Example of SAXS diffractogram (experimental data on NM105 suspension sonicated at pH 2 as circles) illustrating the unified fit (solid red line) and its components, prevailing in each q-domain (dashed-dotted lines, see text for details). Insert of transmission electronic micrograph (credit CODA-CERVA) illustrating the gyration radius of primary particles (Rg1) and aggregates (Rg2) used in the model.

The sum of these two regimes (**Fit primary** in Figure D 6) would describe scattering intensity resulting from individual uncorrelated primary particles, *i.e.* if they were perfectly dispersed and non-aggregated. It prevails in the large q range (domain III, Figure D 6). The upturn of the intensity at small q is due to the association of primary particles into aggregates of finite size.

These aggregates also present a finite size and inner structure. Thus, a second Guinier regime is associated with the structural size of aggregates and prevails in the domain I defined in the Figure D 6:

$$I_{Guinier\,2}(q) = G_2 \exp\left(\frac{-q^2 Rg_2{}^2}{3}\right)$$

The prefactors G_1 and G_2 are defined by:

$$G_i = N_i(\Delta\rho)^2 V_i^2$$

where N_i and V_i are respectively the number density and volume of object i (primary particle or aggregate).

XXXI

These two Guinier regimes give access to the radii of gyration of the primary particles, Rg_1 and of the aggregates, Rg_2.

The ratio of G1 to B1 is a measure of the anisotropy of the primary particles since

$$\frac{G_1}{B_1} \alpha \frac{V^2}{2\pi S}$$

, with V the volume of the particles and S their surface.

For intermediate q range between the scale of aggregates and the scale of primary particles (domain II in the Figure D 6), the intensity decays with a slope typical for the fractal regime of an aggregate and described by a power-law linked to the mass-fractal dimension D_f:

$$I_{Fractal}(q) = B_2\, q^{-D_f}$$

The prefactor B_2 is linked to D_f, G_2 and Rg_2 by:

$$B_2 = \frac{G_2}{Rg_2{}^{D_f}} D_f \Gamma\left(\frac{D_f}{2}\right)$$

Γ standing for the gamma function. (5)

The fractal dimension D_f is a measure of the degree of ramification and density of aggregates (value between 1 and 3).(9)

An average number of primary particles per aggregate can be derived from the Guinier prefactors:

$$N_{part/agg} = \frac{G_2}{G_1}$$

The global unified fit is obtained by the addition of the different terms.(6)

To fit the experimental diffractograms, the total model curve

$$I(q) = I_{Porod\,1}(q) + I_{Guinier\,1}(q) + I_{Fractal}(q) + I_{Guinier\,2}(q)$$

Is plotted and parameters (B_1, G_1, G_2, D_f, Rg_1 and Rg_2) are adjusted manually so that the model fits the best the experimental data. Three parameters are there to describe the primary particles, and three are also necessary to describe the aggregates structures of primary particles. It can be noted that in TEM three independent parameters were also required to describe the aggregates.

Some geometrical restrictions have to be respected ($D_f < 3$; volume of N primaries < volume of aggregate, total surface area of primaries cannot be smaller than the corresponding surface area for ideal spheres).

All SAXS data are treated to be represented in the absolute scale (intensity in cm^{-1}). Therefore quantitative measurements are accessible and through the use of the invariant theorem (10) it is possible to calculate the exact concentration of samples, and then correlate the specific surface area

XXXII

developed in the suspension to the specific surface area of raw materials obtained from powder samples.

V. Comments on use and applicability

VI. References

1. T. Zemb, O. Taché, F. Né, and O. Spalla; "A high-sensitivity pinhole camera for soft condensed matter"; JOURNAL OF APPLIED CRYSTALLOGRAPHY, 36, 800-805, **2003**.
2. F. Né, I. Grillo, O. Taché, and T. Zemb. ; "From raw image to absolute intensity: Calibration of a guinier-mering camera with linear collimation"; JOURNAL DE PHYSIQUE IV, 10(P10), 403-413, **2000**.
3. O. Spalla, S. Lyonnard, and F. Testard; "Analysis of the small-angle intensity scattered by a porous and granular medium"; JOURNAL OF APPLIED CRYSTALLOGRAPHY, 36, 338-347, **2003**.
4. J. Lambard, P. Lessieur and Th. Zemb ; "A triple axis double crystal multiple reflection camera for ultra small angle X-ray scattering"; JOURNAL DE PHYSIQUE I FRANCE, 2 , 1191-1213, **1992**. Lambard, J.; Lesieur, P.; Zemb, T., A triple axis double crystal multiple reflection camera for ultra small angle X-ray scattering. J. Phys. I France 1992, 2 (6), 1191-1213.
5. O. Taché ; « Une architecture pour un système évolutif de contrôle commande d'expériences de physique », Engineer thesis, 2006, available at http://iramis.cea.fr/sis2m/lions/tango/tango-ds/memoire.pdf
6. Beaucage, G., Small-Angle Scattering from Polymeric Mass Fractals of Arbitrary Mass-Fractal Dimension. Journal of Applied Crystallography 1996, 29 (2), 134-146.
7. Kammler, H. K.; Beaucage, G.; Mueller, R.; Pratsinis, S. E., Structure of Flame-Made Silica Nanoparticles by Ultra-Small-Angle X-ray Scattering. Langmuir 2004, 20 (5), 1915-1921.
8. Kammler, H. K.; Beaucage, G.; Kohls, D. J.; Agashe, N.; Ilavsky, J., Monitoring simultaneously the growth of nanoparticles and aggregates by in situ ultra-small-angle x-ray scattering. Journal of Applied Physics 2005, 97 (5), 054309-11.
9. Hyeon-Lee, J.; Beaucage, G.; Pratsinis, S. E.; Vemury, S., Fractal Analysis of Flame-Synthesized Nanostructured Silica and Titania Powders Using Small-Angle X-ray Scattering. Langmuir 1998, 14 (20), 5751-5756.
10. Bushell, G. C.; Yan, Y. D.; Woodfield, D.; Raper, J.; Amal, R., On techniques for the measurement of the mass fractal dimension of aggregates. Advances in Colloid and Interface Science 2002, 95 (1), 1-50.
11. Porod, G.; Glatter, O.; Kratky, O., General theory : Small-angle X-ray scattering. Academic Press ed.; Academic Press: New York, 1982.

XXXIII

Appendix E: Data and parameters determined by unified fit model for SAXS on TiO_2 and synthetic amorphous silica suspensions

I. TiO_2 suspensions in acidic medium

TiO_2 NM	NM102	NM103	NM104	NM105
Rg_1 (Angstrœm)	64	130	130	130
G_1	33	140	122.5	135
B_1	7.20E-06	7.00E-06	7.00E-06	5.63E-06
Rg_2 (Angstrœm)	2800	700	800	650
G_2	660000	15750	21000	350000
D_f	3	2.2	2.3	2.45
B_2	0.001	0.519	0.271	0.100
$N_{part/agg}$	20000.0	112.5	171.4	116.7
$V N_{part}/V_{agg}$	0.24	0.72	0.74	0.93
Invariant from fit (cm^{-4})	7.59E+20	1.04E+21	9.44E+20	8.77E+20
Volumic fraction of NM in suspension	6.28E-04	8.58E-04	7.81E-04	7.26E-04
Suspension concentration from invariant (g/L)	2.66	3.63	3.31	3.07
Specific surface in suspension from Porod (m^{-1}) ($S_{particles}/V_{suspension}$)	1.87E+05	1.82E+05	1.82E+05	1.46E+05
Specific surface of NM from invariant and Porod (m^2/g)	70.41	50.08	55.01	47.60
Theorethical concentration from weighing (g/L)	3.39	3.49	3.42	3.39
Specific surface area of NM determined by SAXS on powder	65.6	51.1	52.4	47

Appendix F: DLS main size parameters of repeated samples of TiO$_2$ and SAS in their best dispersed state for vial homogeneity assessment

Z-average, polydispersity index, position of the main peak in intensity distribution and width of this peak, mean values for multiple samples and standard deviations (SD), extracted from DLS results performed on samples from a given vial number by a given partner. Samples measured by SAXS also are in italic.

I. TiO$_2$ suspensions in acidic medium

NM10X	partner	vial n°	repetition /date	Z-Average	(SD)	PdI	(SD)	Intensity distribution main peak	(SD)	FWHM main peak	(SD)
NM102	CEA	34	20110719	533.3		0.486		964.5		796.3	
NM102	*CEA*	*34*	*20110802*	*377.9*		*0.419*		*587.4*		*417.3*	
NM102	CEA	34	20110729	380.3		0.352		622.5		362.8	
NM102	CEA	34	20111006	478.8		0.455		633.6		264.7	
intra vial				**442.6**	**76.6**	**0.428**	**0.058**	**702.0**	**176.1**	**460.3**	**232.7**
NM102	CEA	35	20110328	403.1		0.411		695.8		373.9	
NM102	CEA	24	20111123	400.4		0.441		654.8		493.2	
NM102	CEA	31	20111207	389.5		0.426		685.4		572.4	
inter vial (4-CEA)				**408.9**	**23.2**	**0.427**	**0.012**	**684.5**	**21.0**	**474.9**	**82.2**
all				**423.3**	**59.4**	**0.427**	**0.042**	**692.0**	**125.8**	**468.7**	**174.7**
NM103	CEA	47	20100927	112.1		0.244		139.2		72.34	
NM103	CEA	47	20110718	115.7		0.253		137.9		69.33	
NM103	*CEA*	*47*	*20110722*	*113.6*		*0.258*		*139.5*		*80.34*	
intra vial				**113.8**	**1.8**	**0.252**	**0.007**	**138.9**	**0.9**	**74.0**	**5.7**
NM103	CEA	557	20110729	117.3		0.212		148		78.1	
NM103	CEA	557	20110915	112.6		0.255		141.4		86.51	
NM103	CEA	557	20110930	108		0.229		124.5		54.81	
intra vial				**112.6**	**4.7**	**0.232**	**0.022**	**138.0**	**12.1**	**73.1**	**16.4**
NM103	INRS	576	N1	138.7		0.244		123.06			
NM103	INRS	576	N2	133.7		0.202		117.52			
NM103	INRS	576	N3	124.4		0.115		117.52			
intra vial				**132.3**	**7.3**	**0.187**	**0.066**	**119.4**	**3.2**		
inter vial all (3)				**119.6**	**11.0**	**0.224**	**0.033**	**132.1**	**11.0**	**73.6**	**0.6**
all				**119.6**	**10.5**	**0.224**	**0.045**	**132.1**	**11.4**	**73.6**	**11.0**

NM10X	partner	vial n°	repetition /date	Z-Average	(SD)	PdI	(SD)	Intensity distribution main peak	(SD)	FWHM main peak	(SD)
NM104	CEA	39	20110119	127.7		0.220		166		88.14	
NM104	CEA	39	20110214	128.8		0.224		172.4		103.6	
intra vial				**128.3**	**0.8**	**0.222**	**0.003**	**169.2**	**4.5**	**95.9**	**10.9**
NM104	CEA	465	20110722	130.6		0.226		169		90.98	
NM104	CEA	465	20110907	127.1		0.218		164.8		87.49	
NM104	*CEA*	*465*	*20110929*	*129*		*0.216*		*156.7*		*74.69*	
intra vial				**128.9**	**1.8**	**0.220**	**0.005**	**163.5**	**6.3**	**84.4**	**8.6**
NM104	NRCWE	803		124.6		0.204		160		80.14	
NM104	NRCWE	885		129.6		0.229		166.9		91.18	
NM104	NRCWE	1157	-1	125.9		0.220		161.8		85.44	
NM104	NRCWE	1157	-2	125.4		0.201		159.4		81.09	
NM104	NRCWE	1157	-3	123.5		0.196		155		74.55	
NM104	NRCWE	1157	-4	127.9		0.220		167.2		89.37	
NM104	NRCWE	1157	-5	124		0.211		158.7		82.98	
intra vial				**125.3**	**1.7**	**0.210**	**0.011**	**160.4**	**4.5**	**82.7**	**5.5**
inter vial (3-NRCWE)				**126.5**	**2.7**	**0.214**	**0.013**	**162.4**	**3.9**	**84.7**	**5.8**
inter vial all (5)				**127.3**	**2.2**	**0.217**	**0.010**	**164.0**	**4.0**	**86.9**	**6.5**
all				**127.0**	**2.3**	**0.215**	**0.010**	**163.2**	**5.3**	**85.8**	**8.0**
NM105	NRCWE	2758		135.6		0.134		156.5		61.83	
NM105	NRCWE	2749		127.9		0.145		151.4		63.85	
NM105	NRCWE	2701		127.8		0.143		150.7		61.86	
inter vial (3-NRCWE)				**130.4**	**4.5**	**0.141**	**0.006**	**152.9**	**3.2**	**62.5**	**1.2**
NM105	INRS	2194	N1	131.7		0.061		141.29			
NM105	INRS	2194	N2	134.0		0.052		134.93			
intra vial				**132.9**	**1.6**	**0.057**	**0.006**	**138.1**	**4.5**		
NM105	CEA	2176	20111123	130.1		0.170		158.1		72.26	
NM105	CEA	305	20100209	128		0.162		155.1		69.71	
NM105	CEA	305	20101006	120.7		0.192		152.4		74.72	
NM105	CEA	305	20101011	121.6		0.189		153.3		73.72	
NM105	*CEA*	*305*	*20110705*	*122.7*		*0.143*		*143.1*		*58.42*	
NM105	CEA	305	20110928	129.3		0.172		156.2		69.59	
intra vial				**124.5**	**3.9**	**0.172**	**0.020**	**152.0**	**5.2**	**69.2**	**6.5**
inter vial all (6)				**129.8**	**4.0**	**0.137**	**0.042**	**151.1**	**7.0**	**65.8**	**4.7**
all				**128.1**	**4.7**	**0.142**	**0.044**	**150.3**	**7.1**	**67.3**	**5.8**

Co-funded by the Health Programme of the European Union

II. *Silica suspensions in pure water*

NM20X	partner	vial n°	repetition /date	Z-Average	(SD)	PdI	(SD)	Intensity distribution main peak	(SD)	FWHM main peak	(SD)
NM200	CEA	50	20101005	222		0.435		244.4		158.8	
NM200	CEA	50	20110202	198.5		0.371		218.1		115.3	
NM200	CEA	50	20110922	195.6		0.343		226.7		134.9	
NM200	*CEA*	*50*	*20111116*	*212.4*		*0.412*		*262.9*		*230*	
	intra vial			**207.1**	**12.3**	**0.390**	**0.041**	**238.0**	**19.9**	**159.8**	**50.1**
NM200	CEA	95	20111129	195.3		0.378		222.4		163.1	
NM200	INRS	109	N1	238.54		0.246		338.93			
NM200	INRS	109	N2	243.04		0.244		281.91			
NM200	INRS	109	N3	239.9		0.255		257.11			
	intra vial			**240.5**	**2.3**	**0.248**	**0.006**	**292.7**	**42.0**		
NM200	NRCWE	279		183.2		0.244		215		109.6	
NM200	NRCWE	494		184.8		0.237		226.3		125.8	
NM200	NRCWE	372		176.6		0.232		215.9		114.6	
	inter vial (3-NRCWE)			**181.5**	**4.3**	**0.238**	**0.006**	**219.1**	**6.3**	**116.7**	**8.3**
	inter vial all (6)			**197.9**	**23.4**	**0.288**	**0.075**	**235.0**	**29.4**	**134.6**	**25.2**
	all			**208.2**	**24.4**	**0.309**	**0.079**	**246.3**	**37.8**	**144.0**	**40.1**
NM201	*CEA*	*48*	*20110922*	*232.5*		*0.371*		*315.3*		*215.2*	
NM201	CEA	48	20110202	183.7		0.332		173.7		65.69	
	intra vial			**208.1**	**34.5**	**0.352**	**0.028**	**244.5**	**100.1**	**140.4**	**105.7**
NM201	CEA	39	20111129	185.9		0.323		183.7		70.73	
	inter vial			**197.0**	**15.7**	**0.337**	**0.020**	**214.1**	**43.0**	**105.6**	**49.3**
	all			**200.7**	**27.6**	**0.342**	**0.026**	**224.2**	**79.0**	**117.2**	**84.9**
NM202	CEA	1	20110202	179.1		0.356		158.6		54.1	
NM202	*CEA*	*1*	*20111115*	*172.7*		*0.354*		*161.1*		*58.2*	
	intra vial/all			**175.9**	**4.5**	**0.355**	**0.001**	**159.9**	**1.8**	**56.2**	**2.9**

NM20X	partner	vial n°	repetition /date	Z-Average	(SD)	PdI	(SD)	Intensity distribution main peak	(SD)	FWHM main peak	(SD)
NM203	CEA	207	20110720	166.4		0.409		178.1		90.51	
NM203	*CEA*	*207*	*20111115*	*179.4*		*0.444*		*183.8*		*74.52*	
intra vial				**172.9**	**9.2**	**0.427**	**0.025**	**181.0**	**4.0**	**82.5**	**11.3**
NM203	CEA	118	20110202	179.2		0.375		154.5		63.88	
NM203	INRS	227	N1	218.93		0.29		141.29			
NM203	INRS	227	N2	288.17		0.327		154.92			
NM203	INRS	227	N3	230.05		0.281		147.95			
intra vial				**245.7**	**37.2**	**0.299**	**0.024**	**148.1**	**6.8**		
NM203	NRCWE	294		146.3		0.214		183.1		83.6	
NM203	NRCWE	212		146.6		0.229		181.7		83.36	
NM203	NRCWE	169	-1	142.2		0.219		169.7		77.46	
NM203	NRCWE	169	-2	149.9		0.247		189.6		99.09	
NM203	NRCWE	169	-3	152.4		0.259		181.3		84.68	
NM203	NRCWE	169	-4	145.6		0.25		171.6		76.53	
intra vial				**147.5**	**4.5**	**0.244**	**0.017**	**178.1**	**9.2**	**84.4**	**10.4**
inter vial (3-NRCWE)				**146.8**	**0.6**	**0.229**	**0.015**	**181.0**	**2.6**	**83.8**	**0.6**
inter vial all (6)				**173.0**	**38.4**	**0.298**	**0.086**	**171.1**	**15.5**	**79.6**	**8.8**
all				**178.8**	**45.1**	**0.295**	**0.077**	**169.8**	**16.1**	**81.5**	**10.1**

Co-funded by
the Health Programme
of the European Union

● Contact ●

Website:
www.nanogenotox.eu

E-mail:
nanogenotox@anses.fr

Coordinator: French Agency for Food, Environmental and Occupational Health & Safety (ANSES)

27-31, avenue du Général Leclerc
94701 Maisons-Alfort Cedex
France

Partners

French Agency for Food, Environmental and Occupational Health Safety (France)	ANSES	
Federal Institute of Risk Assessment (Germany)	BfR	
French Atomic Energy Commission (France)	CEA	
Institute of Mineralogy and Crystallography (Bulgaria)	IMC-BAS	
Veterinary and Agrochemical Research Centre (Belgium)	CODA-CERVA	
Finnish Institute of Occupational Health (Finland)	FIOH	
Roumen Tsanev Institute of Molecular Biology Academy of Sciences (Bulgaria)	IMB-BAS	
Institut national de recherche et de sécurité (France)	INRS	
National Health Institute Doutor Ricardo Jorge (Portugal)	INSA	
Scientific Institute of Public Health (Belgium)	IPH	
Institut Pasteur of Lille (France)	IPL	
Istituto superiore di sanità (Italy)	ISS	
The Nofer institute of Occupational Medicine (Poland)	NIOM	
National Research Centre for the Working Environment (Denmark)	NRCWE	
National Institute for Public Health and the Environment (The Netherlands)	RIVM	
Universitat Autònoma de Barcelona (Spain)	UAB	

Co-funded by
the Health Programme
of the European Union

Grant Agreement n° 2009 21 01